UNCLASSIFIED

MARTIN MARIETTA ENERGY SYSTEMS LIBRARIES
3 4456 0050904 6

ORNL-940, Series A
Progress Report
Physics

PHYSICS DIVISION
QUARTERLY PROGRESS REPORT FOR
PERIOD ENDING DECEMBER 20, 1950

OAK RIDGE NATIONAL LABORATORY
CENTRAL RESEARCH LIBRARY
DOCUMENT COLLECTION
LIBRARY LOAN COPY
DO NOT TRANSFER TO ANOTHER PERSON
If you wish someone else to see this document, send in name with document and the library will arrange a loan.
UCN-7969
(3 3-67)

OAK RIDGE NATIONAL LABORATORY
OPERATED BY
CARBIDE AND CARBON CHEMICALS DIVISION
UNION CARBIDE AND CARBON CORPORATION
UCC
POST OFFICE BOX P
OAK RIDGE, TENNESSEE

UNCLASSIFIED

UNCLASSIFIED

ORNL 940

This document consists of 54 pages
Copy 9 of 230, Series A

Contract No. W-7405, eng 26

PHYSICS DIVISION

A. H. Snell, Director
E. O. Wollan, Associate Director

QUARTERLY PROGRESS REPORT
for Period Ending December 20, 1950

Edited by:
M. E. Rose

DATE ISSUED: MAR 15 1951

OAK RIDGE NATIONAL LABORATORY
operated by
CARBIDE AND CARBON CHEMICALS DIVISION
Union Carbide and Carbon Corporation
Post Office Box P
OAK Ridge, Tennessee

UNCLASSIFIED

MARTIN MARIETTA ENERGY SYSTEMS LIBRARIES
3 4456 0050904 6

INTERNAL DISTRIBUTION

1. G. T. Felbeck (C&CCD)
2-3. Chemistry Library
4. Physics Library
5. Biology Library
6. Health Physics Library
7. Metallurgy Library
8-9. Training School Library
10-13. Central Files
14. C. E. Center
15. C. E. Larson
16. W. B. Humes (K-25)
17. W. D. Lavers (Y-12)
18. A. M. Weinberg
19. J. A. Swartout
20. E. D. Shipley
21. E. J. Murphy
22. F. C. VonderLage
23. A. H. Snell
24. E. H. Taylor
25. A. Hollaender
26. K. Z. Morgan
27. F. L. Steahly
28. M. T. Kelley
29. W. H. Pennington
30. E. O. Wollan
31. D. W. Cardwell
32. A. S. Householder
33. L. D. Roberts
34. J. A. Lane
35. M. M. Mann
36. R. N. Lyon
37. W. C. Koehler
38. W. K. Ergen
39. E. P. Blizard
40. M. E. Rose
41. M. J. Skinner
42. G. E. Boyd
43. Lewis Nelson
44. R. W. Stoughton
45. C. E. Winters
46. W. H. Jordan
47. E. C. Campbell
48. D. S. Billington
49. M. A. Bredig
50. R. S. Livingston
51. C. P. Keim
52. J. L. Meem
53. G. H. Clewett
54. C. D. Susano
55-64. Central Files (O.P.)

EXTERNAL DISTRIBUTION

65-76. Argonne National Laboratory
77. Armed Forces Special Weapons Project
78-83. Atomic Energy Commission, Washington
84. Battelle Memorial Institute
85. Brush Beryllium Company
86-89. Brookhaven National Laboratory
90. Bureau of Medicine and Surgery
91. Bureau of Ships
92-95. Carbide and Carbon Chemicals Division (K-25 Plant)
96. Columbia University (J. R. Dunning)
97. Columbia University (G. Failla)
98-102. E. I. du Pont de Nemours and Company
103-106. General Electric, Richland
107-110. Idaho Operations Office
111-112. Iowa State College
113. Kansas City Operations Branch
114. Kellex Corporation
115-116. Kirtland Air Force Base
117-120. Knolls Atomic Power Laboratory
121-123. Los Alamos Scientific Laboratory
124. Mallinckrodt Chemical Works
125. Massachusetts Institute of Technology (A. Gaudin)
126. Massachusetts Institute of Technology (A. R. Kaufmann)
127-129. Mound Laboratory
130. National Advisory Committee for Aeronautics
131. National Bureau of Standards (R. D. Huntoon)
132. Naval Medical Research Institute
133-134. Naval Radiological Defense Laboratory
135. New Brunswick Laboratory
136-138. New York Operations Office

139. North American Aviation, Inc.
140-143. Carbide and Carbon Chemicals Division (Y-12)
144. Patent Branch, Washington
145. RAND Corporation
146. Sandia Corporation
147. Santa Fe Operations Office
148-162. Technical Information Service, Oak Ridge
163-165. USAF, NEPA Office
166. Savannah River Operations Office, Wilmington
167-168. U. S. Geological Survey (T. B. Nolan)
169-170. U. S. Public Health Service
171. University of California at Los Angeles
172-176. University of California Radiation Laboratory
177-178. University of Rochester
179. University of Washington
180. Western Reserve University
181-184. Westinghouse Electric Corporation
185. Yale University
186-189. Atomic Energy Project, Chalk River
190. Chief of Naval Research
191. H. K. Ferguson Company
192. Harshaw Chemical Company
193. Isotopes Division (Mr. McCormick)
194-195. Library of Congress, Acquisition Department (J. W. Cormn)
196. National Bureau of Standards
197. National Research Council, Ottawa
198. Naval Research Laboratory
199-200. Nevis Cyclotron Laboratories
201. Nucleonics
202-203. Oak Ridge Institute of Nuclear Studies
204-213. United Kingdom Scientific Mission (M. Greenhill)
214. USAF, Eglin Air Force Base (Technical Library)
215. USAF, Wright-Patterson Air Force Base (Rodney Nudenberg)
216-220. USAF, Wright-Patterson Air Force Base (CADO)
221. U. S. Army, Army Field Forces (Captain James Kerr)
222. U. S. Army, Atomic Energy Branch (Lt. Col. A. W. Betts)
223. U. S. Army, Director of Operations Research (Dr. Ellis Johnson)
224. U. S. Army, Office, Chief of Ordnance (Col. A. R. Del Campo)
225-226. U. S. Army, Office of the Chief Signal Officer (Curtis T. Clayton thru Major George C. Hunt)
227-229. U. S. Army, Technical Command (Col. J. H. Rothschild Attn: Technical Library)
230. UT-AEC Agricultural Research Program (Charles S. Hobbs)

TABLE OF CONTENTS

INTRODUCTION AND SUMMARY 5

PUBLICATIONS 8

1. NEUTRON DIFFRACTION 9

Scattering Cross Sections of Nitrogen 9

Polarization of Bragg-reflected Neutrons from Ferromagnetic Crystals 10

2. NUCLEAR ALIGNMENT PROGRAM 12

Hafnium Superconductivity 14

Neutrons and Superconductivity 15

3. SHORT-PERIOD ACTIVITIES 16

Radiations from the 2.5-sec Activity in Erbium 16

Decay Scheme for Ag^{108} 19

Spectrum of Ag^{110} 22

4. SHORT-LIVED ISOMERS 25

5. INVESTIGATIONS WITH THE SCINTILLATION SPECTROMETER 30

Long-lived Cadmium 30

$Iodine^{131}$ 30

Hollow-crystal Spectrometer 36

6. ACCELERATOR PROGRAM 40

7. STABLE-ISOTOPE CROSS SECTIONS 43

8. NEUTRON ELECTRIC DIPOLE MOMENT 45

9. THEORETICAL PHYSICS 46

A Theory of Radiation Widths of Slow-neutron Resonances 46

The De Groot-Tolhoek Symmetry Principle in Beta Decay 50

Elastic Scattering of Atoms by Atoms 52

10. HEAVY ION RESEARCH 53

LIST OF FIGURES

Fig. 1	Scintillation Spectra of 2.5-sec Erbium	17
Fig. 2	Scintillation Spectrum of Ag^{108} β-rays; Anthracene Crystal	20
Fig. 3	Fermi Plot of β Spectrum of Ag^{108}; Anthracene Crystal	21
Fig. 4	Scintillation Spectrum of Ag^{108} γ-rays; NaI Crystal. Inset: Proposed Decay Scheme for Ag^{108}	23
Fig. 5	Coincidence Rate vs. Delay Time for Decay of Re^{186}	26
Fig. 6	Comparison of Data and Computed Delayed Coincidence Counting Rate Curves for Os^{186} Decay	28
Fig. 7	Decay of Cd^{113}	31
Fig. 8	Gamma-ray Spectrum of I^{131}	33
Fig. 9	Decay Scheme of I^{131}	34
Fig. 10	Split-crystal Gamma Scintillation Spectrometer Arrangement for Beta-Gamma Coincidences	35
Fig. 11	Fermi Plot of I^{131} Beta Decay	37
Fig. 12	P^{32} Spectrum with Hollow Crystal Spectrometer	39
Fig. 13	Relative Intensity of Gamma Rays from Protons on B^{11}	41
Fig. 14	Angular Distribution of Gammas in Selected Energy Range	42

INTRODUCTION AND SUMMARY

This report covers unclassified work of the Physics Division for the period September 20 to December 20, 1950. The classified section of the Physics Division Quarterly Report appears separately (ORNL-939).

The additions to the research staff in the Physics Division are Drs. M. K. Wilkinson (Neutron Diffraction), L. A. Rayburn (Neutron Diffraction), S. Tamor (Theoretical Physics), H. B. Willard (Accelerator Group), and P. M. Stier (Heavy Ion Research).

Neutron Diffraction. Utilizing the fact that electronic and nuclear scattering are very nearly equal in the (220) reflection from Fe_3O_4 it has been possible to obtain neutron beams with essentially 100% polarization. It has also been demonstrated that the Fe_3O_4 lattice shows antiferromagnetic coupling.

The coherent and total scattering cross sections of N^{14} have been measured and their approximate equality (9.1 and 10.3 barns) shows weak spin dependence of the nuclear forces in this case.

Nuclear Alignment Program. Preparations are being made to utilize the 100% polarized neutron beams to detect possible changes in the manganese cross section due to nuclear alignment. An a-c field is being utilized to flip the direction of the polarized neutron spins. Measurements of the entropy of manganous ammonium sulfate as a function of field and temperature have been carried out as an aid in determining the degree of nuclear alignment. According to preliminary results, hafnium shows no superconductivity in the region $0.16 < T < 4.2$, contrary to the results of Kürti and Simon. Further investigation with hafnium of higher degree of purity is planned.

Short-period Activities. From internal conversion measurements the 205-Kev γ from erbium (2.5 sec) has been classified as (most probably) electric dipole or quadrupole, in serious conflict with the interpretation resulting from half-life data. β- and γ-ray studies in the decay of Ag^{108} have been made and a decay scheme has been proposed. Confirmation of Siegbahn's assignment of the 24-sec period to the ground state of Ag^{110} has been obtained.

Short-lived Isomers. The half-life of the isomeric state of $_{76}Os^{186}$, which emits a 137-Kev γ, has been measured and found to be 8×10^{-10} sec. Both the half-life and internal conversion data are consistent with electric quadrupole radiation.

Physical Electronics. *Long-lived Cadmium.* The half-life of the long-period activity in Cd^{113} has been remeasured. The new value, 3.5 ± 0.5 years, necessitates a change in the activation cross section to 0.20 ± 0.01 barn.

Iodine^{131}. Data from γ-γ and β-γ spectra lead to a consistent decay scheme with three β-chains leading from I^{131} to the ground state of Xe^{131} via the emission of six γ rays. The Fermi plot for the β's in coincidence with the high-energy γ's, after correction for 80-Kev radiation, is fairly straight and gives an end point of 255 ± 10 Kev.

Hollow-crystal Spectrometer. Preliminary results obtained seem to promise satisfactory performance in reducing distortion due to extraneous radiation as well as reduction of scattering losses.

Acceleration Program. Improvements in pulse-height selector, collimator, and monitoring of the beam energy have been effected and the γ-ray spectrum from protons bombarding B^{11} has been obtained. The angular distribution of the γ's in the neighborhood of one of the peaks in the spectrum shows definite anisotropy.

Stable Isotope Cross Sections. Thermal-neutron cross sections have been measured with the pile oscillator for a total of 22 stable isotopes of the elements Mg, Si, Ti, Se, and Te.

Neutron Electric Dipole Moment. The upper limit on the effective charge separation (neutron moment divided by electron charge) has been reduced to 3×10^{-19} cm by recent results.

Theoretical Physics. A simple and admittedly crude model has been used in an attempt to account for γ-ray widths as observed in slow-neutron resonances. The widths as calculated for magnetic dipole and electric quadrupole are in reasonable agreement with observations but the electric dipole widths are too large by a factor of about 10^5. This would be understandable if for some reason electric dipole emission could not occur.

The problem of possible restrictions on the β-decay interaction has been studied with the following results: (1) The symmetry in the $\beta^{\pm}$ spectra in the

absence of a Coulomb field is automatically ensured by the Lorentz invariance of the β-decay Hamiltonian and does not have to be postulated *ad hoc* as was done by Tolhoek and De Groot; and (2) the restriction on the choice of interactions made by Tolhoek and De Groot has no real foundation and is unnecessarily restrictive.

The elastic scattering of atoms by atoms has been set up as a classical orbit calculation. Numerical work is in progress.

Heavy-ion Research. Progress in instrumentation (rebuilding of ion source and construction of target assembly) is reported.

PUBLICATIONS

The following contributions by members of the Physics Division have appeared in the open literature during the period September 30 to December 30, 1950:

1. "A Study of the Slowing Down Distribution of Sb^{124}-Be Photo-neutrons in Graphite, and of the Use of Indium Foils," L. D. Roberts, J. E. Hill, and G. McCammon, *Phys. Rev.* **80**, 6-10 (Oct. 1, 1950).

2. "A 3×10^{-9}-sec Isomeric State in $_{63}Eu^{153}$," F. K. McGowan, *Phys. Rev.* **80**, 482-483 (Nov. 1, 1950).

3. "Photo-Disintegration Cross Sections of Deuterium and Beryllium for the Gamma Rays of Sodium 24 and Gallium 72," A. H. Snell, E. C. Barker, and R. L. Sternberg, *Phys. Rev.* **80**, 637-642 (Nov. 15, 1950).

4. "A 1.7×10^{-9}-sec Isomeric State in $_{68}Er^{166}$," F. K. McGowan, *Phys. Rev.* **80**, 923-924 (Dec. 1, 1950).

1. NEUTRON DIFFRACTION

C. G. Shull E. O. Wollan
W. C. Koehler

Scattering Cross Sections of Nitrogen. Measurements of the total and coherent scattering cross sections of nitrogen obtained from neutron diffraction studies of ZrN have been reported in ORNL-159. The values reported at that time, 4.6 and 6 barns, respectively, for the coherent and total scattering cross sections, were suspect because of impurities in the samples. It was found that the samples contained a large metal impurity, for which corrections were made. Since these results, if accepted, imply a strong spin dependence of scattering for nitrogen, it seemed important to obtain better samples of nitrogen containing crystals and to repeat the measurement. Accordingly, D. LaValle of the Chemistry Division prepared for us a pure sample of potassium trinitride in ample quantity for neutron-diffraction work.

Potassium trinitride is tetragonal with a = 6.094 A and C = 7.056 A. The four molecules of the unit cell all lie in the special positions[1] listed below:

4 K in $0, 0, \frac{1}{4}$; $0, 0, \frac{3}{4}$; $\frac{1}{2}, \frac{1}{2}, \frac{3}{4}$; $\frac{1}{2}, \frac{1}{2}, \frac{1}{4}$

4 N in $0, \frac{1}{2}, 0$; $\frac{1}{2}, 0, 0$; $0, \frac{1}{2}, \frac{1}{2}$; $\frac{1}{2}, 0, \frac{1}{2}$

8 N in $u, u + \frac{1}{2}, 0$; $\frac{1}{2} - u, u, 0$; $u + \frac{1}{2}, u, \frac{1}{2}$; $u, \frac{1}{2} - u, \frac{1}{2}$;

$\bar{u}, \frac{1}{2} - u, 0$; $u + \frac{1}{2}, \bar{u}, 0$; $\frac{1}{2} - u, u, \frac{1}{2}$; $\bar{u}, u + \frac{1}{2}, \frac{1}{2}$

with u = 0.135. Although this would ordinarily be an inconveniently large cell for the application of neutron diffraction techniques, the structure factors are such that five reflections are well resolved. In addition, the ratio of three nitrogen centers to one potassium is favorable to the determination of the nitrogen cross section.

From the observed intensities in the (110), (002), (200), (112), and (211) reflections and the previously measured scattering amplitude of 0.35×10^{-12} cm for potassium, the scattering amplitude for nitrogen is 0.851×10^{-12} cm, corresponding to a cross section of 9.1 barns.

(1) Wyckoff, R. W. G., *Crystal Structure*, Interscience, New York, 1948.

Transmission measurements on the same substance, after correction for absorption, lead to a total scattering cross section of 10.3 barns for nitrogen. Within the limits of the accuracy of the total cross section, little spin incoherence is indicated. These values are in accord with the results of A. W. MacReynolds, whose gas-scattering experiments (ORNL-782) were inconsistent with the previously reported lower values. We have also recently learned of a measurement, as yet unpublished, at the Chalk River Laboratory which is in agreement with the value of 9.1 barns.

Polarization of Bragg-reflected Neutrons from Ferromagnetic Crystals. In the last quarterly report a preliminary report was made on the polarization produced in the neutrons scattered from ferromagnetic crystals. Some measurements on the degree of polarization produced in neutron scattering from an iron crystal (4% Si) were discussed, and it was shown that the polarization analysis was rather sensitive to grain size and orientation effects in the analyzing blocks. Since then we have obtained analyzing blocks of small grain size and with essentially no orientation and we have looked at the polarization produced in the (220) Fe_3O_4 reflection as well as that in the (110) Fe reflection. Theoretically the former should be 100% polarized and the latter 60% polarized according to the measured nuclear and magnetic scattering amplitudes for these reflections.

A thin slice of Fe_3O_4, approximately 1 sq cm in area and 0.1 cm in thickness, was cut along the (220) planes in a natural single crystal of magnetite. This slice was magnetized in the gap of a permanent magnet (H = 4500 oersteds) and a monochromatic beam of neutrons (λ = 1.204 A) was reflected from the (220) planes with the crystal slice set in transmission orientation and with the magnetization vector perpendicular to the plane of scattering. The degree of polarization in the reflected beam was determined by passage through an analyzing block of polycrystalline iron which could be magnetized with a field of 8000 oersteds in the gap of an electromagnet. Single transmission measurements were made of the analyzing block with the analyzing field off and on (with field always parallel to the polarizing field in order to avoid any depolarization of the neutron beam in the intervening space) for both the polarized beam from Fe_3O_4 and for an unpolarized beam from a copper crystal. These measurements permit evaluation of the degree of polarization after allowance for depolarization effects in the analyzing block according to the formulas of Halpern and Holstein. Analysis of the data showed the polarization in the (220) Fe_3O_4 reflection to be 100% within the experimental uncertainty of

perhaps 5%. This means that the relative intensities of the two neutron spin states are in a ratio of at least 40 to 1.

Other crystal reflections are of interest as possible polarizing reflections. Some reflections from cobalt have very favorable amplitudes for this purpose, but this material is difficult to magnetize and internal depolarization of the beam may result. The (110) reflection from an Fe crystal is not too favorable for polarization purposes since by calculation the expected polarization is only about 60%. We have studied this reflection with an Fe crystal (4% Si) in the same fashion as for Fe_3O_4 described above and find it to be about 41% polarized. This lower than calculated value could be explained on the basis of extinction effects, depolarization, or silicon impurity within the crystal lattice.

The (220) Fe_3O_4 reflection is also interesting because *the polarization direction is just reversed from that obtained in the (110) Fe reflection.* This shows up in the sign of the single transmission effect in the analyzing block and results because only Fe^{3+} ions at tetrahedral positions in the magnetic lattice contribute to the intensity in the (220) Fe_3O_4 reflection. The iron atoms at the tetrahedral positions are coupled antiferromagnetically to those at the octahedral positions, and, since the latter are in the majority and consequently will be aligned in the applied field direction, the tetrahedral ions will be aligned antiparallel to the external field. The polarization observation constitutes direct proof of the antiferromagnetic nature of the Fe_3O_4 lattice. Other Fe_3O_4 reflections, also highly polarized, are normal with respect to showing polarization parallel to the applied field direction.

It is possible by this method to produce a collimated beam of monochromatic, completely polarized neutrons with an intensity of about 10^5 neutrons/sec. The beam can also be pulsed since the magnetization vector in crystals of the ferrite series can be twisted around by high-frequency magnetic-field application.

2. NUCLEAR ALIGNMENT PROGRAM

S. Bernstein J. W. T. Dabbs, Jr.
L. D. Roberts C. P. Stanford
T. E. Stephenson*

In the last two quarterly reports[1,2] an experiment was described for the observation of nuclear alignment in manganous ammonium sulfate. A total of six experiments of this type were performed with inconclusive results, but they did demonstrate that the experiment was a practical one. To simplify the equipment used, measurement of the temperature of the manganous ammonium sulfate and strong attempts to obtain maximum neutron polarization were not attempted. Since temperature measurements were not made, it is not certain that the manganous ammonium sulfate sample remained cold (~0.2°K) during the entire activation of about 3 hr. Either a warming of the sample or a small polarization could account for the smallness of the observed effect.

The logical next steps were then to install temperature measuring equipment and to increase the neutron polarization to the maximum possible value. As described in the last quarterly report,[3] nuclear alignment is observed as a change in effective cross section of the aligned maganese nuclei when the sample is activated with polarized as compared to unpolarized neutrons. This observed change of cross section would be doubled if the aligned manganese nuclei were activated first with neutrons polarized with parallel orientation and then with antiparallel orientation. Work has been proceeding along each of these lines.

The design of the temperature-measuring equipment presented some mechanical problems which have now been solved, and shop work on this apparatus is essentially complete; it will soon be installed.

In the above work, the neutrons were polarized by transmission through magnetized iron. However, recent work by Shull and Wollan has demonstrated

* Ralph Allen, an ORINS fellow from the University of Texas, has been added to the group.

(1) Bernstein, S., Roberts, L. D., Dabbs, J. W. T., Jr., Capehart, J. B., Stephenson, T. E., and Stanford, C. P., "Alignment of Nuclei," *Physics Division Quarterly Progress Report for Period Ending June 15, 1950*, ORNL-782, p. 64 (Oct. 4, 1950).

(2) Roberts, L. D., Dabbs, J. W. T., Jr., Stephenson, T. E., Bernstein, S., Stanford, C. P., and Cochran, L. W., "Neutron Physics and Low Temperatures, Nuclear Alighment," *Physics Division Quarterly Progress Report for Period Ending September 20, 1950*, ORNL-865, p. 32 (Jan. 8, 1951).

(3) Bernstein *et al; op. cit.*, ORNL 782; Roberts *et al., op. cit.*, ORNL 865.

that much larger neutron polarizations may be obtained in beams reflected from a magnetized magnetite crystal, and work along this line is being pursued.

The magnetite crystal mentioned in the last quarterly report has been cut. The section we are working with at present is 4 mm thick and has a face area of 12 sq cm. The (220) planes form the two crystal faces. The crystal is mounted in the polarizing magnet so that the magnetic field is parallel to the (100) direction. Preliminary tests using the Bragg reflected beam from the (220) planes have produced a monoenergetic beam of about 5×10^5 neutrons/min with high polarization. Study of the crystal is continuing.

In order to reverse the direction of neutron polarization in the neutron beam, as mentioned above, the beam is subjected to an alternating magnetic field perpendicular to a steady magnetic field after the fashion of Bloch and of Ramsey and Purcell. The oscillator frequency is determined by the strength of the steady magnetic field, and the amplitude of the oscillating magnetic field is determined by the time spent by the neutrons in this oscillating field. When the oscillating field is of proper frequency and strength, the neutrons will absorb enough energy from the field to flip over or reverse their polarization. Preliminary tests were made of the equipment with a partially polarized heterogeneous-energy neutron beam. Results indicated the need of increased amplitude in the a-c magnetic field. Tests will continue with more oscillator power, monoenergetic neutrons, and higher neutron polarization.

In the last two quarterly reports measurements of the entropy of manganous ammonium sulfate in the temperature region below 1°K were discussed. The results were in approximate agreement with appropriate theory; however, the study extended down to a minimum temperature of 0.6°K only, and it was necessary to introduce a surprisingly small value of the Debye characteristic temperature. In the past quarter these measurements of the entropy have been considerably extended, some 30 demagnetizations having been made covering the temperature region from 4.2 to 0.15°K and a magnetic field region from zero to 6000 oersteds. The Debye characteristic temperature has been determined as 146 ± 3°K, which is a quite reasonable value. All measurements in the region covered are consistent within our experimental accuracy (1 to 5%, depending on region) with the expression, in cgs units,

$$S = R \ln 6 - \frac{a}{2T^2} + 232R\left(\frac{T}{\theta}\right)^3 - \frac{A}{2}\left(\frac{H}{T}\right)^2$$

where

$a = 0.033R$ (specific heat constant)

$\theta = 146°K$

$A = 4.34$ (Curie constant)

R = gas constant.

The T - T^* correlation of Cooke[4] was used.

The above entropy function would be expected to hold rigorously only at such values of (H, T) at which saturation effects are negligible ($H/T < 1000$ oersteds/degree and $T > 0.3°K$). However, as mentioned above, we find that this function describes these results even to H/T as large as 6000 oersteds/degree and T as low as 0.15°K. This circumstance permits the calculation of nuclear alignment obtainable from an adiabatic partial demagnetization from H/T values as high as 6000 oersteds/°K to the critical field $H_k^1 = \sqrt{a/A} \approx 800$ oersteds. Assuming the hyperfine structure coupling given by Bleaney,[5] this calculation yields a value for the fraction of nuclei aligned of 0.08. It is expected that demagnetizations from higher initial values of H/T (e.g., 2×10^4 oersteds/degree) will yield larger values of nuclear alignment, perhaps by a factor of 2. The above entropy function could not possibly be expected to fit in such a case; apparatus is therefore being built to measure directly the electron magnetic moment, the absolute temperature, and thus the entropy as a function of final magnetic field for these more extreme initial conditions. In addition to the above, Dr. Albert Simon and Dr. M. E. Rose, of the Theoretical Physics Group, have kindly consented to calculate the partition function for manganous ammonium sulfate based on the constants given by Bleaney. This will give valuable additional information on optimum demagnetization conditions for maximum nuclear alignment and will provide the necessary theoretical interpretation for the above experimental program.

Hafnium Superconductivity. In 1935, Kürti and Simon[6] demonstrated that hafnium is a superconductor with a zero-field transition at 0.35 ± 0.05°K.

(4) Cooke, A. H., "The Estsblishment of the Absolute Scale of Temperature Below 1°K," *Proc. Phys. Soc.* A62, 269 (1949).

(5) Bleaney, B., "Nuclear Specific Heats in Paramagnetic Salts," *Phys. Rev.* 78, 214 (1950).

(6) Kürti, N., and Simon, F. E., "Experiments at Very Low Temperatures. Obtained by the Magnetic Method. II. New Supraconductors," *Proc. Roy. Soc. London* A151, 610 (1935).

However, they did not determine the transition temperature as a function of applied magnetic field. Because hafnium has the lowest transition temperature of any superconductor, and because it is desirable to determine this magnetic field—transition temperature relation, equipment has been set up for this study. A sample* (2 cc) consisting of chromium potassium alum (1.8 cc) and hafnium metal (0.2 cc) was pressed, and the susceptibility-temperature relation in zero field was investigated as a preliminary step. A total of seven demagnetizations were made using this hafnium, covering the temperature range of 0.16 to 0.7°K. No transition was observed in the susceptibility-temperature curve, and the minimum temperature reached on demagnetization agreed, within experimental error, with the value obtained with samples of pure chromium potassium alum of the same volume and shape and under as nearly the same initial conditions as could be obtained. In view of the above, and the fact that no susceptibility anomaly was found between 1.1 and 4.2°K, it may be concluded that this sample shows no superconductivity in the region 0.16 to 4.2°K. This hafnium metal was prepared by a chemical reduction process, and, since superconductivity phenomena are very sensitive to sample purity, it seems that, even with the thorough annealing, its purity (chemical or physical) was not sufficient. The sample used by Kürti and Simon was prepared by the hot-wire technique of Van Arkel and De Boer, and, although it may have had a higher zirconium content than our sample, it was undoubtedly more pure in every other respect. It is planned to obtain a hafnium sample prepared by this hot-wire technique and continue this investigation.

Neutrons and Superconductivity. Beams of unpolarized and partially polarized neutrons were passed through a cylindrical sample of tin at temperatures above and below its superconducting transition temperature of 3.69°K, and the transmission through a magnetized iron analyzer was measured. No measurable change in either polarization or transmission was observed when the sample went through the superconducting transition. These results would perhaps permit certain conclusions to be drawn regarding domains inside a superconductor, but since the neutron polarization used was rather modest, these conclusions should await repetition of the experiment with a more highly polarized beam.

* This sample was kindly furnished by Paul J. Hagelston, of Y-12, and was annealed 42 hr at 1000°C and 8×10^{-6} mm Hg.

3. SHORT-PERIOD ACTIVITIES

E. C. Campbell

Radiations from the 2.5-sec Activity in Erbium (Max Goodrich,* E. C. Campbell, and J. H. Kahn). The radiations from samples of erbium oxide, activated for a few seconds in the Oak Ridge Graphite Reactor by means of a fast pneumatic tube, have been investigated with a recording scintillation spectrometer. The complete pulse-height spectrum was recorded photographically within about 5 sec after the irradiation was completed. No measurable activity (i.e., greater than a few percent of the total) was found other than the 2.5-sec period first reported by Der Mateosian and Goldhaber.[1]

Readings, approximately proportional to the differential counting rate, plotted as a function of pulse height, were obtained from the photographs by means of a special microphotometer. Figure 1 shows three such microphotometer records in which the pulse-height scale has been converted to energy by comparison with known radiations. Curve *A*, obtained with 1500 mg/cm^2 of lucite absorber in front of a 1-in. thick sodium iodide (thallium-activated) crystal, exhibits two peaks due to photoelectrons ejected in the crystal by two groups of photons. The more energetic group of photons is assumed to be gamma rays from an isomeric transition in erbium and the less energetic group to be erbium K X-rays resulting from internal conversion for the same transition. The results from several such records give 210 ± 10 Kev and 55 Kev for the two photon groups.

Results consistent with these have been found in a study of the internal conversion spectrum. Curve *B* shows, to a different energy scale, the spectrum obtained with an anthracene crystal when no absorber is used. If the two broad peaks at about 125 and 175 Kev are due to conversion electrons from the K and L shells, respectively, the transition energy, after correcting for a small amount of absorption, is about 205 Kev. Since it was necessary to have a sample thickness of at least 1 mg/cm^2 to give sufficient counts for a photograph, self-absorption made the resolution extremely poor. Nonetheless, some half-dozen such curves gave an average of 200 Kev with a mean deviation of about 10 Kev. The uncertainty in the correction for the absorption and in the location of the poorly resolved peaks suggests, however, that the results are somewhat less reliable than those obtained with the sodium iodide crystal.

* Research Participant, Oak Ridge Institute of Nuclear Studies; on leave from Department of Physics, Louisiana State University.

(1) Mateosian, E. der, and Goldhaber, M., "Nuclear Isomers Produced by Slow Neutron Capture" (Abstract), *Phys. Rev.* 76, 187 (1949).

UNCLASSIFIED
DWG. 9555

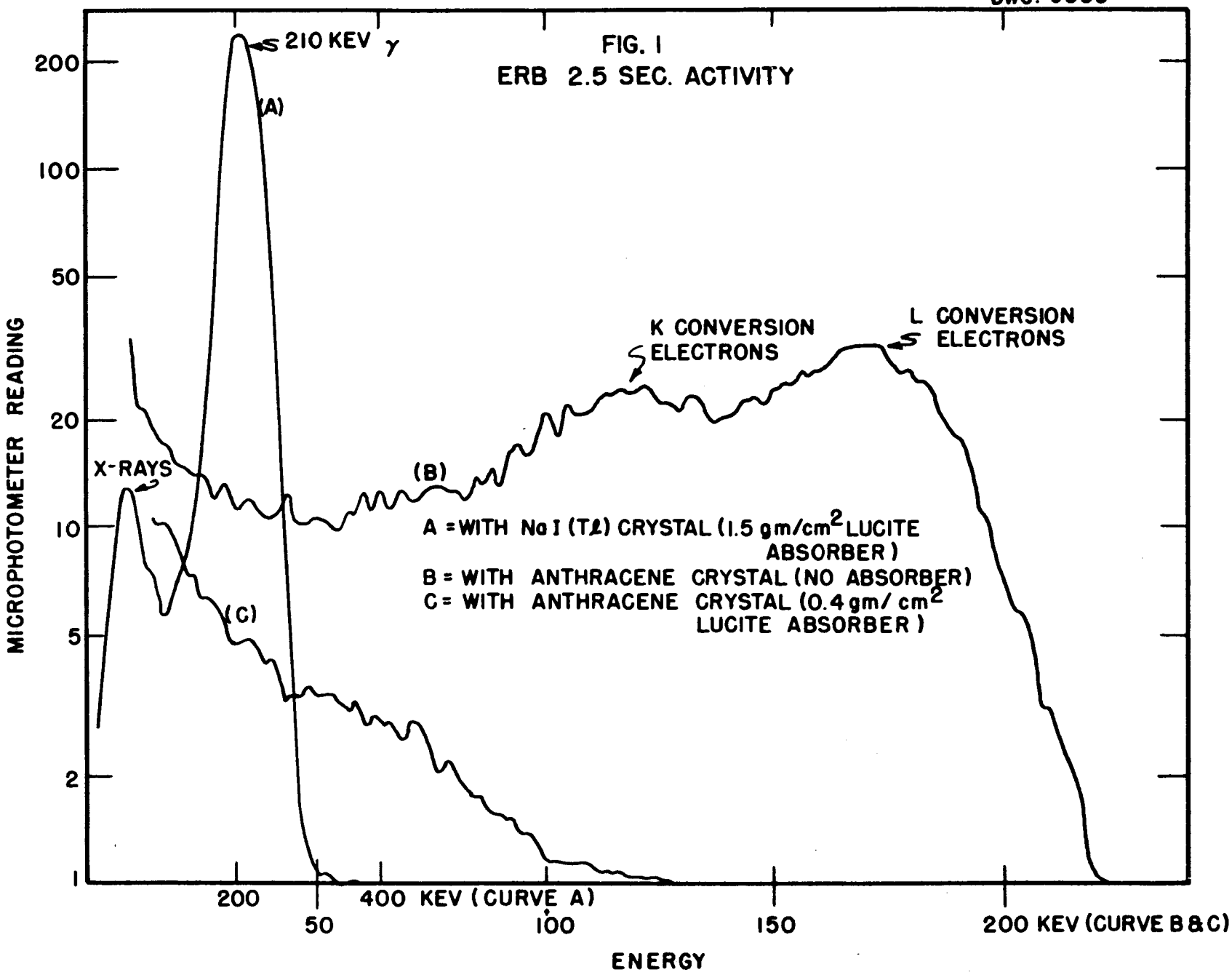

If it is assumed that the low-energy peak of curve *A* is due entirely to K X-rays from internal conversion, and that the detection efficiency of the crystal is the same for the two groups of photons (the efficiency is known to approach 100% in this energy region for the 1-in.-thick crystal), an experimental value for the K conversion coefficient can be obtained. For each of the several curves taken, N_e/N_γ was found in this way to be in the region of 0.05 to 0.10. According to the calculated conversion coefficients of Rose *et al.*,[2] electric dipole and electric quadrupole radiations of energy $0.4mc^2$ have coefficients of 0.041 and 0.153, respectively, for $Z = 67$. The coefficients for the corresponding magnetic radiations are 0.34 and 1.62. For $Z = 68$ the coefficients would be only slightly different since the dependence on Z is small. The results found indicate, therefore, that the radiation is electric dipole or possibly electric quadrupole and disagree seriously with the published[3,4] multipole order of 4 as determined from the lifetime of the excited state.

The explanation of the disagreement is not clear. The calculations of Rose require N_e/N_γ to be 1.65 and 26, respectively, for electric and magnetic radiation of multipole order 4. The lower one of these is more than ten times the observed ratio of the number of K X-rays to the number of gamma rays. The effect both of Auger processes and of differential absorption in the lucite would be to make the observed number of X rays too small, but the production of Auger electrons at such high Z is known to be quite small, and measurements with absorbers of different thickness as well as calculations from X-ray absorption tables show that the X rays are absorbed only a few percent more than the gamma rays. It should be mentioned that order of magnitude estimates of α_K from the curves *B* and *C* agree roughly with the values found from the X rays. The area under the K conversion electron peak of curve *B* is about four times as great as the area under the gamma-ray curve *C*. For a conversion coefficient of approximately 2 (required for $l = 4$ transition), a detection efficiency of 50% would have to be assumed for the 2.5-mm-thick anthracene crystal, whereas X-ray absorption tables indicate that the efficiency is provably only a few percent. Thus the evidence all points toward a

(2) Rose, M. E., Goertzel, G., Spinrad, B., Harr, J., and Strong, P., private communication.

(3) Mateosian and Goldhaber, *op. cit.*

(4) Axel, P., and Dancoff, S. M., "Classification of Nuclear Isomers," *Phys. Rev.* 76, 892 (1949).

real discrepancy between the multipole order determined from the lifetime and that determined from the conversion coefficient. It is possible that the decay may not be simple. If the nucleus first decays from the metastable level to a level only a few Kev below it and then to the ground state, values can be assigned which more nearly resolve the difficulty.

Decay Scheme for Ag^{108} (Max Goodrich). The radiation from 2.4-min silver first found by Fermi and his collaborators[5] has been widely listed in nuclear tables, from cloud-chamber measurements made in 1936,[6] as a beta-ray of 2.8 Mev end point. No observation of gamma rays is listed. In view of the improvement of techniques since that time, it seemed desirable to make new measurements of these radiations.

Samples of natural $AgNO_3$ were irradiated in the Oak Ridge Graphite Reactor by use of a fast pneumatic tube for known times from a few seconds up to a few minutes. After irradiation, the samples were placed in an inactive holder, allowed to decay for a known time of from 5 to 10 min, and examined with a scintillation spectrometer. Readings were taken with a single-channel differential analyzer at half-minute intervals, corrections being made for decay at the 2.4-min half-life rate. When, owing to the decay of the sample, the background became an appreciable fraction of the activity, the readings were stopped, the sample was allowed to decay to background, and a new irradiation of the same length of time was made. The readings were then continued with some overlap of points. A logarithmic count-rate meter monitored the total radiation and provided a check that the activity was sensibly the same after each irradiation.

Measurements made on a sample about 10 mg/cm^2 in thickness using an anthracene crystal as phosphor are shown in Fig. 2 and reproduced in a Fermi plot in Fig. 3. Two beta rays are clearly evident with end points at 0.83 and 1.47 Mev. The "feet" on the points of Fig. 2 were obtained with the statistics alone, no estimate of the error due to extrapolation for decay being included. Because of the difficulties of the method, the uncertainty in the end points is at least 0.05 Mev. No beta ray higher in energy than the 1.47 Mev exists to more than a few percent of the total activity.

(5) Amaldi, E., D'Agostino, O., Fermi, E., Pontecorvo, B., Rasetti, F., and Segrè, E., "Artificial Radioactivity Produced by Neutron Bombardment. II." *Proc. Roy. Soc. London* A149, 522 (1935).

(6) Naidu, R., and Siday, R. E., "β-Ray Spectra of Some Induced Radioactive Elements Resulting from Neutron Bombardment," *Proc. Phys. Soc. London* 48, 332 (1936).

UNCLASSIFIED
DWG. 9554

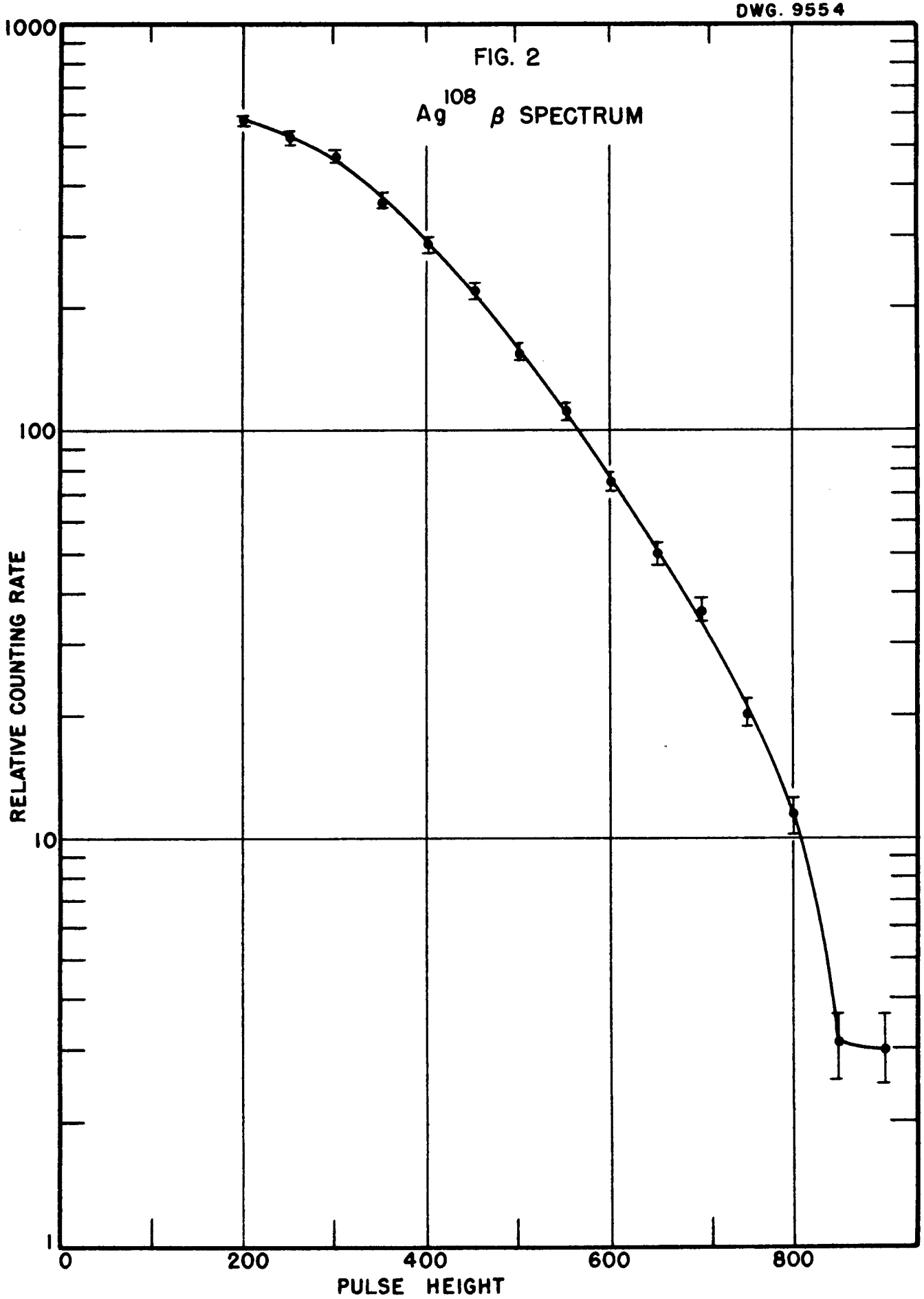

UNCLASSIFIED
DWG. 9518

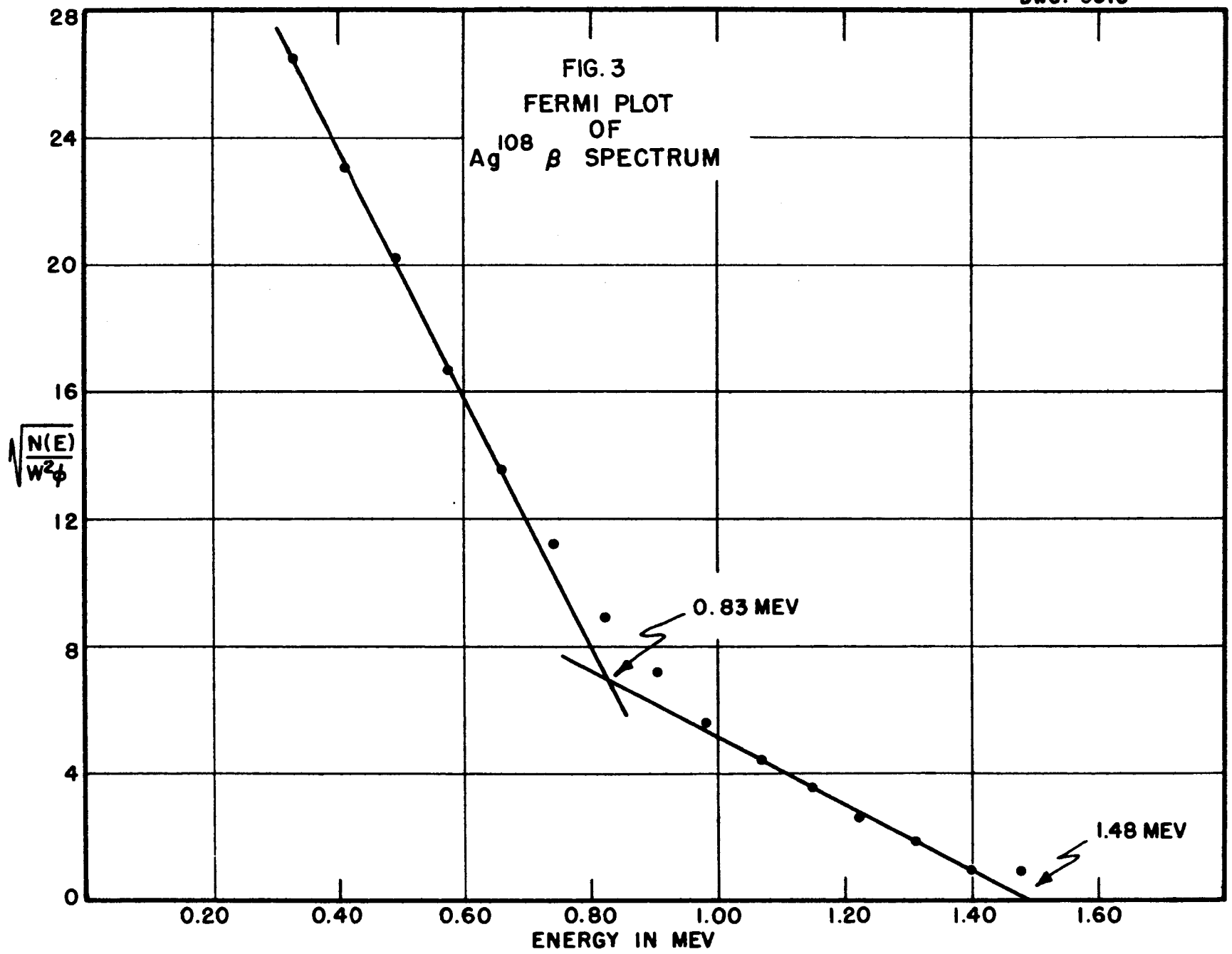

FIG. 3
FERMI PLOT
OF
Ag^{108} β SPECTRUM

The gamma-ray studies were made with a NaI(Tl) crystal as phosphor. A lucite absorber of 2.25 gm/cm^2 thickness was used to stop the beta rays. A source of about 60 mg/cm^2 thickness gave sufficient activity to make the measurements. The data, reproduced in Fig. 4, show photoelectron peaks for gamma rays at 0.615 ± 0.02, 0.420 ± 0.02, and 0.188 ± 0.01 Mev. Using the pulse-height spectrum of the Cs^{137} 0.663-Mev gamma ray (obtained with the same NaI crystal) normalized to fit the 0.615-Mev gamma ray at their photoelectron peaks, the relative contribution of the 0.615-Mev gamma ray was determined. Similarly, the I^{128} 0.428-Mev gamma ray spectrum was used to determine the contribution of the 0.420-Mev gamma ray to the remainder of the total spectrum. When detection efficiencies of the crystal for the gamma rays, estimated from preliminary measurements to be 70, 80, and 100%, in order of decreasing energy, were applied, the relative intensities obtained were, in the same order, 4:1:1.

The proposed decay scheme, shown in the inset of Fig. 4, is consistent with both the energies and the intensities of the radiations observed in this work. The indicated relative intensity of the two beta rays was calculated from the decay scheme and the ratio of total beta rays to total gamma rays as measured with the monitor and agrees approximately with the relative intensities as obtained from the Fermi plot.

Spectrum of Ag^{110} (Max Goodrich). From studies of the radiations of the 225-day silver activity, Siegbahn[7] has proposed a decay scheme in which the activity originates in a metastable level 116 Kev above the ground state. A small complex fraction of the beta radiation, with end points of 2.86 and 2.12 Mev, is placed with its origin in the ground state and is presumed to be the beta radiation of the well-known 24-sec activity. Seigbahn's data suggested that still other low-intensity beta rays may connect the Ag^{110} ground state with excited levels of the Cd^{110} nucleus. Confirmation of the assignment of the 24-sec period to the ground state has been found.[8] Further confirmation is provided in the present work by the measurement of the energies of the beta and gamma rays in the 24-sec activity.

Using a scintillation spectrometer, direct measurement of the spectrum of the short-lived radiations has been made with the fast pneumatic tube installed at the Oak Ridge Graphite Reactor. The apparatus, details of which will be

(7) Siegbahn, K., "The Disintegration of Ag^{110}," *Phys. Rev.* 77, 233 (1950).

(8) Miskel, J., "The Genetic Relationship in Ag^{110}," *Phys. Rev.* 79, 403 (1950).

UNCLASSIFIED
DWG. 9520

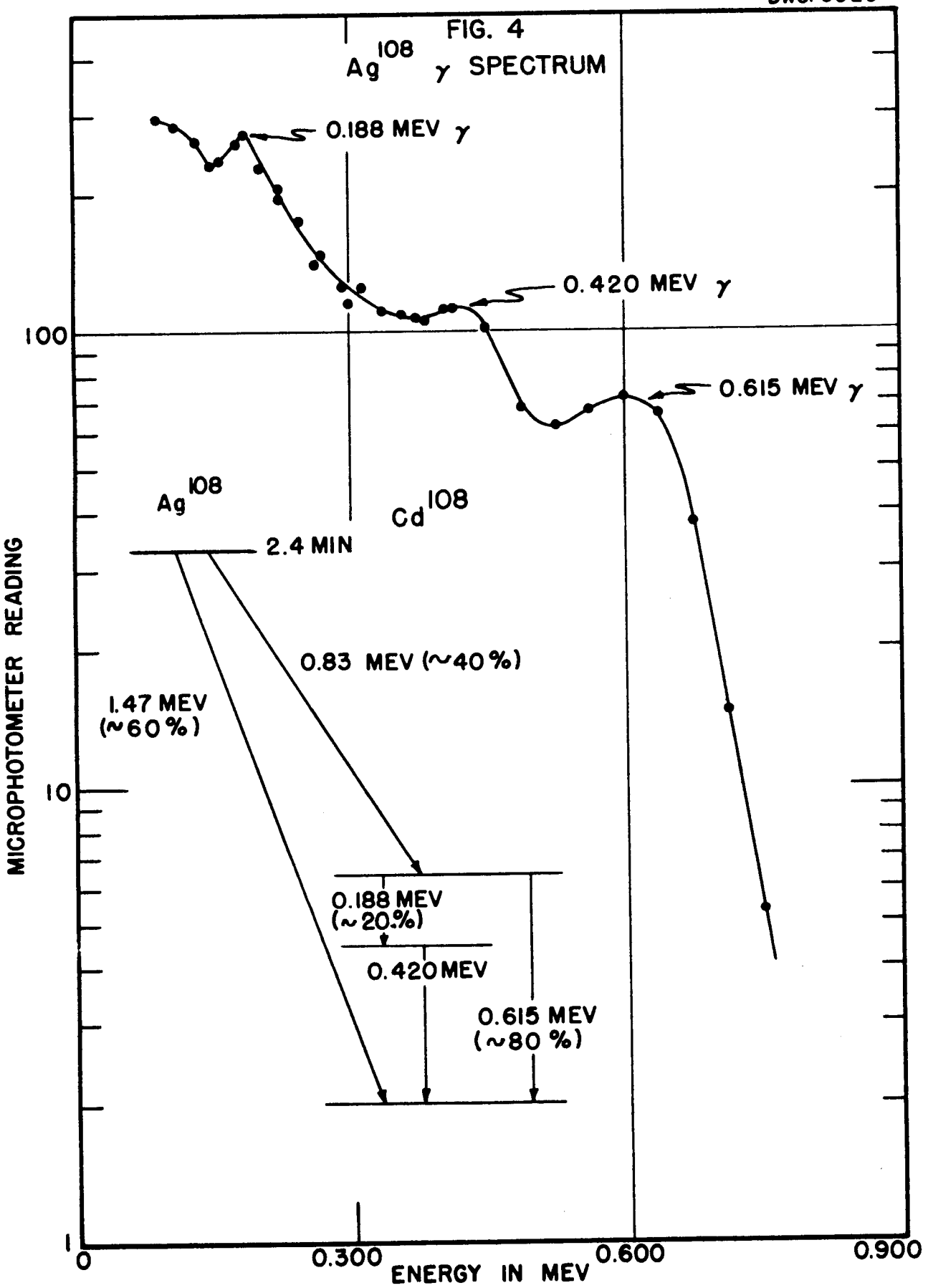

published later, uses a No. 5819 photomultiplier tube with either an anthracene or a NaI(Tl) crystal. The beta-spectrum is complex and has been found by Fermi analysis to contain components having end points of 2.8 ± 0.1 Mev and 2.1 ± 0.2 Mev. The gamma spectrum shows a relatively strong line at 0.66 ± 0.02 Mev, a very much weaker line at about 0.9 Mev, and a suggestion of other extremely weak lines. Within the limits of error, the two beta rays and the strong gamma ray can be identified, respectively, with the 2.86- and 2.12-Mev beta rays and the 0.656-Mev gamma-ray observed by Siegbahn. The gamma ray at about 0.9 Mev is probably the sum of Siegbahn's 0.885- and 0.935-Mev lines. Its presence (5% of the 0.66-Mev line) indicates that the spectrum does contain a weak component going to one of the upper levels of the product nucleus.

The lower energy beta ray constitutes the larger fraction of the total beta-ray activity. Estimates made of this fraction from the extrapolated Fermi plots, and also from the ratio N_β/N_γ along with Siegbahn's decay scheme, gave values of from 60 to 70%.

4 SHORT-LIVED ISOMERS

F. K. McGowan

An excited state in $_{76}Os^{186}$ with a half-life of $(8 \pm 1) \times 10^{-10}$ sec has been observed with the delayed-coincidence scintillation spectrometer. The data have been analyzed by a graphical method which is analogous to a method of analysis recently reported by Newton.[1]

Re^{186} (90 hr) is known to decay in 90% of its disintegrations by β^- emission into Os^{186}.[2] A 25% partial β^- spectrum of 930 Kev end point is followed by a 137-Kev gamma ray, and the remaining β^- disintegrations lead directly to the ground state. For the 137-Kev gamma ray Metzger and Hill measured $\alpha_K = 0.35 \pm 0.1$ and $N_K/N_L = 0.6 \pm 0.1$.

Curve 1 of Fig. 5 shows the number of coincidences as a function of delay time obtained with a source of Re^{186}. This delayed-coincidence resolution curve was recorded by exciting one channel of the delayed-coincidence apparatus by 250- to 450-Kev nuclear beta rays and the other channel by the L and M internal conversion electrons of the 137-Kev transition. Without changing the apparatus a resolution curve for prompt events was obtained with a source of Au^{198}. The prompt coincidences are (1) between 110- to 150-Kev nuclear beta-rays and conversion electrons of the 411-Kev transition and (2) between 110- to 150-Kev Compton recoil electrons from the 411-Kev gamma radiation and 250- to 450-Kev nuclear beta rays. Curve 2 shows the result of such a measurement. Since curves 1 and 2 overlap appreciably, the half-life of Os^{186*} cannot be determined accurately from the slope of curve 1 at a large positive delay time.

Newton[3] has given a general discussion of the evaluation of delayed-coincidence experiments. In the ideal experiment it is desired to excite one channel of the apparatus by the radiation announcing an excited state in a

(1) Newton, T. D., "Decay Constants from Coincidence Experiments," *Phys. Rev.* 78, 490 (1950).

(2) Metzger, F. R., and Hill, R. D., "Disintegration Scheme of Re^{186}," *Bull. Am. Phys. Soc.* 25, Chicago Meeting, Paper E8, p. 12 (1950).

(3) *Op. cit.*

UNCLASSIFIED
DWG. 10174

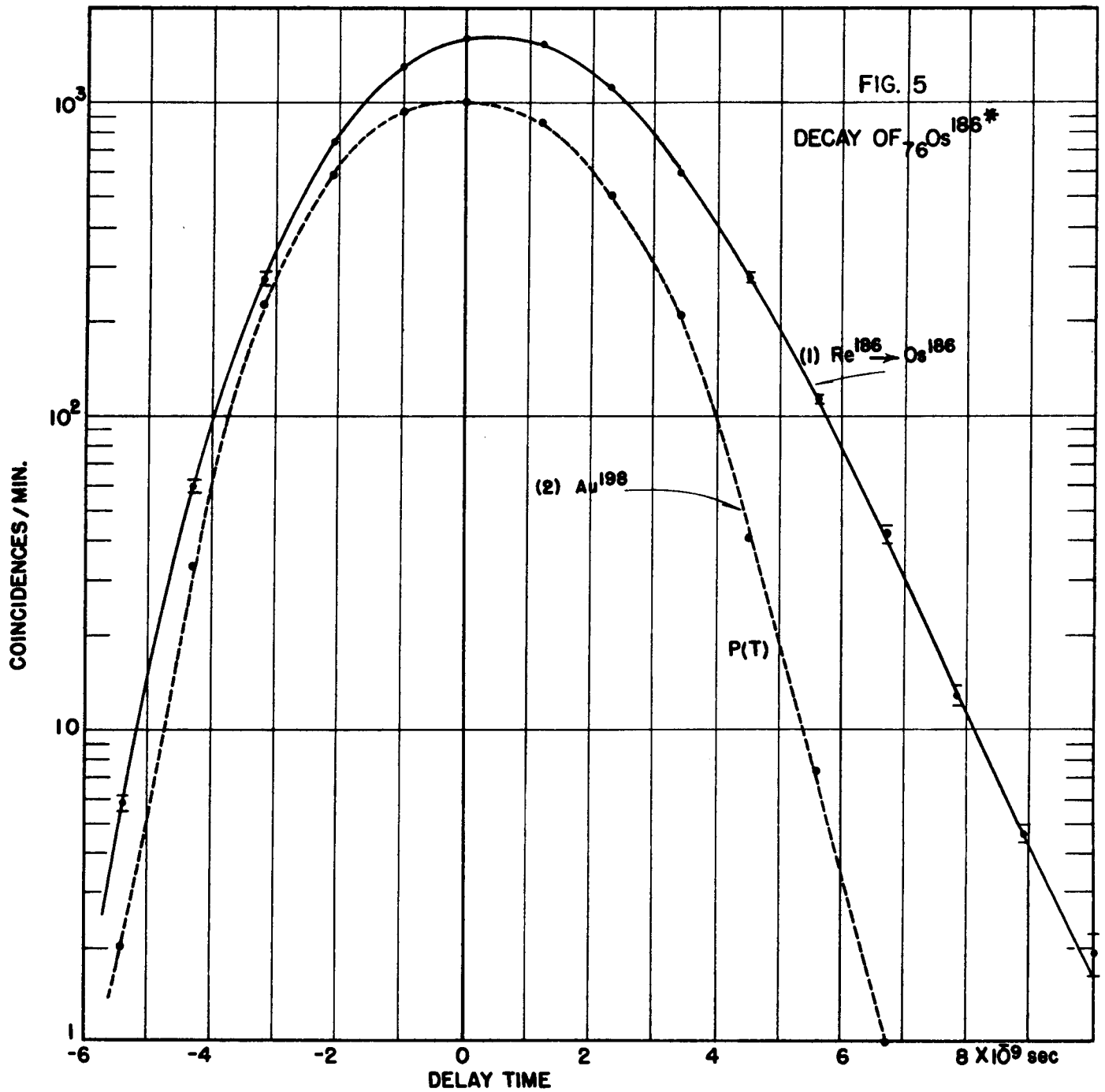

nucleus and to excite the other channel by the radiation emitted in the decay of the excited state where lifetime is to be measured. If the excited state has a lifetime much too short to be measured by the coincidence apparatus, a prompt-coincidence curve $P(T)$ is obtained, where T is the delay time introduced in the delayed-coincidence apparatus. If there is a measurable lifetime a delayed-coincidence resolution curve, $F(T, \lambda)$, is obtained, given by

$$F(T, \lambda) = \int_0^\infty \lambda e^{-\lambda t} P(T - t)\, dt$$

Since the energy resolution of the scintillation spectrometer is relatively poor compared to the best magnetic beta-ray spectrometers, the delayed-coincidence resolution curve in Fig. 5 for $Re^{186} \longrightarrow Os^{186}$ is $F(T, \lambda)$ plus possibly some prompt-event counts not related to the $Re^{186} \longrightarrow Os^{186*}$ decay and prompt events due to scattering from one to the other detector. Prompt events from scattering are, of course, greatly reduced in number when the delayed-coincidence scintillation spectrometer is used.

Delayed-coincidence resolution curves $F(T, \lambda)$ were computed graphically, using for $P(T)$ curve 2 of Fig. 5 and values of λ equal to or near that obtained in the usual way from the slope of curve 1 at a large positive value of T. The prompt curve $P(T)$ represents the response of the apparatus to simultaneous emission of radiation of the same energy that gave curve 1. The computed curves $F(T, \lambda)$ for $T_{1/2} = (9.0, 8.0, \text{ and } 7.0) \times 10^{-10}$ sec are shown in Fig. 6 and have been normalized to the experimental delayed-coincidence resolution curve at $T = 6 \times 10^{-9}$ sec. The agreement between the computed curve for $T_{1/2} = 8.0 \times 10^{-10}$ sec and the experimental curve is exceedingly good. The difference between the two curves for $T < 5 \times 10^{-9}$ sec yields a resolution curve of prompt events not related to the $Re^{186} \longrightarrow Os^{186*}$ decay; the shape of the resulting residual curve agrees with the experimental resolution curve for prompt events of Fig. 5. It appears that the initial state of the 137-Kev gamma-ray transition from Os^{186} is metastable with a half-life of 8.0×10^{-10} sec.

UNCLASSIFIED
DWG. 10175

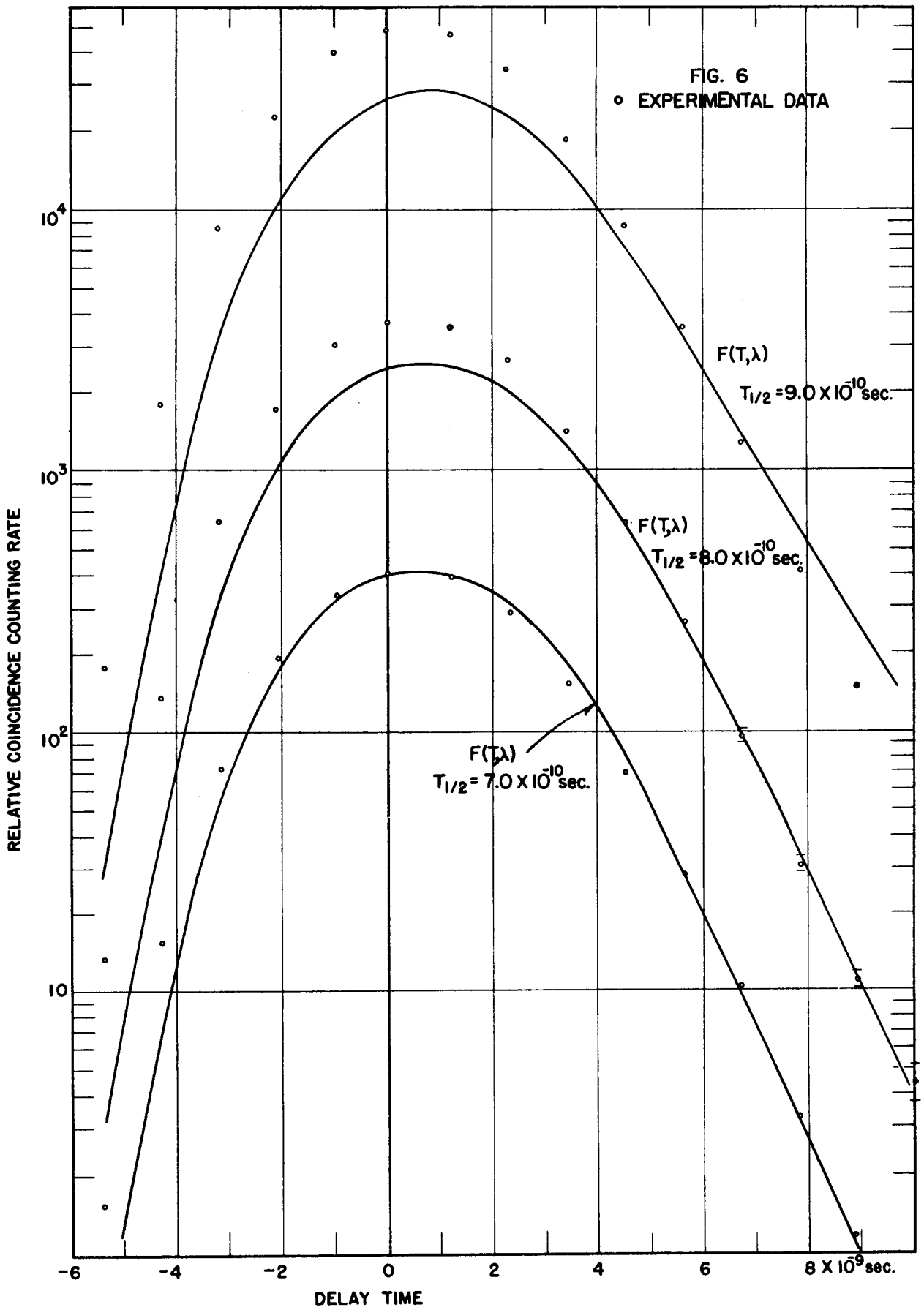

The energy and half-life of this isomeric state suggest that the transition corresponds to forbiddenness $l = 2$. Recently a few relativistic calculations without screening for L_I shell internal conversion[4] have been completed for $Z = 92$, 84, and 49 for electric and magnetic dipole and electric quadrupole radiation. For a gamma-ray energy of 137 Kev and $Z = 84$, the computed ratios $(N_K/N_{L_I})_{el(2)^1\text{-pole}}$, $(N_K/N_{L_I})_{el(2)^2\text{-pole}}$, and $(N_K/N_{L_I})_{mag(2)^1\text{-pole}}$ are 8.5, 2.0, and 19, respectively.[5] Since Metzger and Hill measured $(N_K/N_L) = 0.6$ for the 137-Kev transition in ${}_{76}Os^{186}$, it appears that electric quadrupole radiation occurs.

(4) Gellman, H., Griffith, B. A., and Stanley, J. P., "Internal Conversion in the L_I Shell," *Phys. Rev.* 80, 866 (1950); table of L_I shell internal conversion coefficients, privately circulated; computations performed at the Computation Centre, McLennan Laboratory, University of Toronto.

(5) Rose, M. E., *et al.*, Tables of K-Conversion Coefficients.

5. INVESTIGATIONS WITH THE SCINTILLATION SPECTROMETER

P. R. Bell
J. M. Cassidy
R. C. Davis
G. G. Kelley

Long-lived Cadmium. The long-lived beta emitter identified in the last quarterly report[1] as Cd^{113} has been followed further, and estimates of its half-life have been made. Decay of an old sample measured on a mica-window tube for 83 days gave the results shown in Fig. 7. The straight line was fitted by least squares and gives a half-life of 3.5 years. By fitting lines by eye it would seem that this value could be in error by ±0.5 year at most.

The irradiated Cd^{112} sample described in ORNL-865 shows both the 43-day and the 3.5-year activity when run on the scintillation spectrometer. By measuring the areas, the relative intensities were found at various times. Assuming the shorter half-life to be 43 days, a half-life of 1.9 to 2.3 years for the Cd^{113} results. This value is much less reliable than that found from direct decay measurement since the 43-day activity is still much larger than the 3.5-year at the last measurement. As a consequence of the changed half-life, the cross section estimated in the previous quarterly report must be increased. The isotopic cross section for activation of the 3.5-year activity by thermal neutrons is now 0.020 ± 0.01 barn based upon the 43-day activation cross section of 0.14 barn.

Iodine^{131}. Zeldes, Brosi, and Ketelle of the Chemistry Division have located a gamma ray at 0.72 Mev and the missing 0.9-Mev beta-ray branch leading to the 12-day xenon metastable state. The other five gamma rays from I^{131} are well known. The energies are

	Kev
γ_1	80.1
γ_2	165
γ_3	284
γ_4	364
γ_5	638
γ_6	720

The gamma-gamma and beta-gamma coincidence spectra were run using two scintillation spectrometers in coincidence. NaI-TlI crystals were used for the gamma-gamma runs.

(1) Bell, P. R.; Cassidy, J. M.; and Davis, R. C.; "Split-crystal scintillation Spectrometer." *Physics Division Quarterly Progress Report for Period Ending September 20, 1950*, ORNL-865, p. 21 (Jan. 8, 1951).

UNCLASSIFIED
DWG. 10323

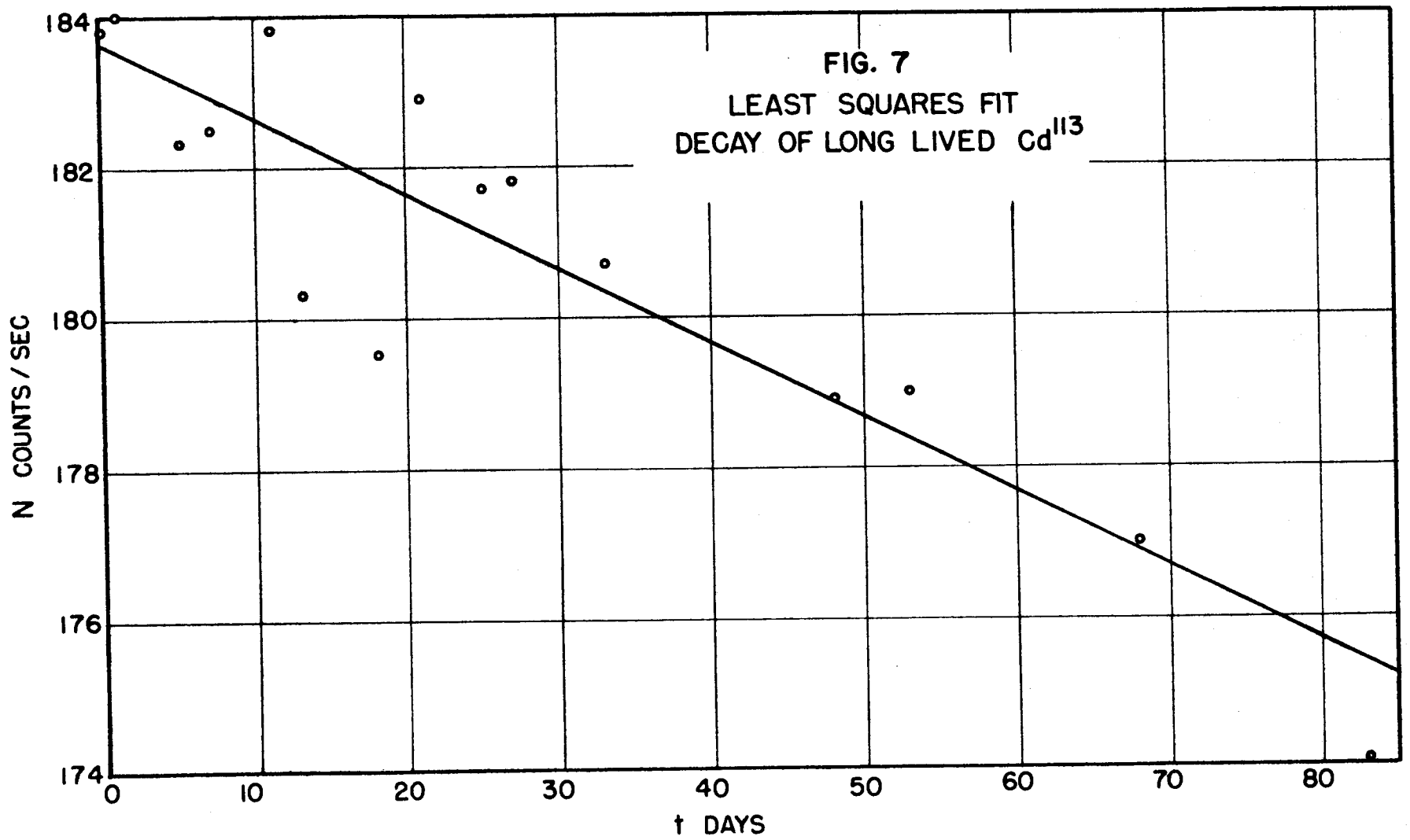

FIG. 7
LEAST SQUARES FIT
DECAY OF LONG LIVED Cd^{113}

Figure 8, curve *A*, shows the gross gamma-ray spectrum given by one of the spectrometers. Figure 8, curve *B*, shows the gross coincidence curve corrected for accidentals. By this is meant the spectrum of pulses in one spectrometer that are coincident with any pulse produced in the other spectrometer. The correction for accidentals, Fig. 8, curve *C*, is obtained by delaying one of the spectrometer pulses sufficiently so that no immediate coincidence can occur. The counts will then all be due to random coincidences. The prominent peak due to the 364-Kev gamma ray is absent from the coincidence curve as well as the weak peak due to the 720-Kev gamma ray. This shows that the 364- and 720-Kev gamma rays are not in coincidence with any other gamma rays. On the other hand the 284-, 638-, and 80-Kev gamma rays are each in coincidence with at least one other of the three.

Figure 8, curve *D*, shows the spectrum of gamma rays coincident with gamma-ray pulses above 525 Kev in the other crystal. The 284-Kev gamma ray is now missing from the spectrum, only the 80-Kev and X-rays remaining. This proves that the 638- and 284-Kev gamma rays are not coincident and that the 80-Kev ray is in coincidence with both the 284- and 638-Kev transitions. The points labeled *E* in Fig. 8 are those found when the second spectrometer is set for coincidences with gamma rays above 675 Kev. The resultant pulses at the higher energy seem to be accounted for by the random background. The counts at the X-ray peak are more than the random background but are probably from beta-ray excited X rays.

The coincidence information leads to a consistent decay scheme, shown in Fig. 9, with no ambiguity. This is essentially the same as that of Kern, Mitchell, and Zaffarano(2) except for the crossover 720-Kev gamma ray which they did not see.

The energy generally reported for the lowest energy beta ray, around 300 Kev, cannot fit this decay scheme because of the well-known gamma-ray energies and the 600-Kev major beta ray. This lower energy beta ray is difficult to measure in magnetic spectrometers and may well be in error.

The split-crystal spectrometer using anthracene was arranged in coincidence with a gamma scintillation spectrometer using NaI as shown in the sketch (approximately to scale) in Fig. 10. The gamma spectrometer was set to produce

(2) Kern, B. D., Mitchell, A. C. G., and Zaffarano, D. J., "The Nuclear Spectra of Sb^{125}, Te^{125*}, Cr^{51}, and I^{131}," *Phys. Rev.* 76, 94 (1949).

UNCLASSIFIED
DWG. 10322

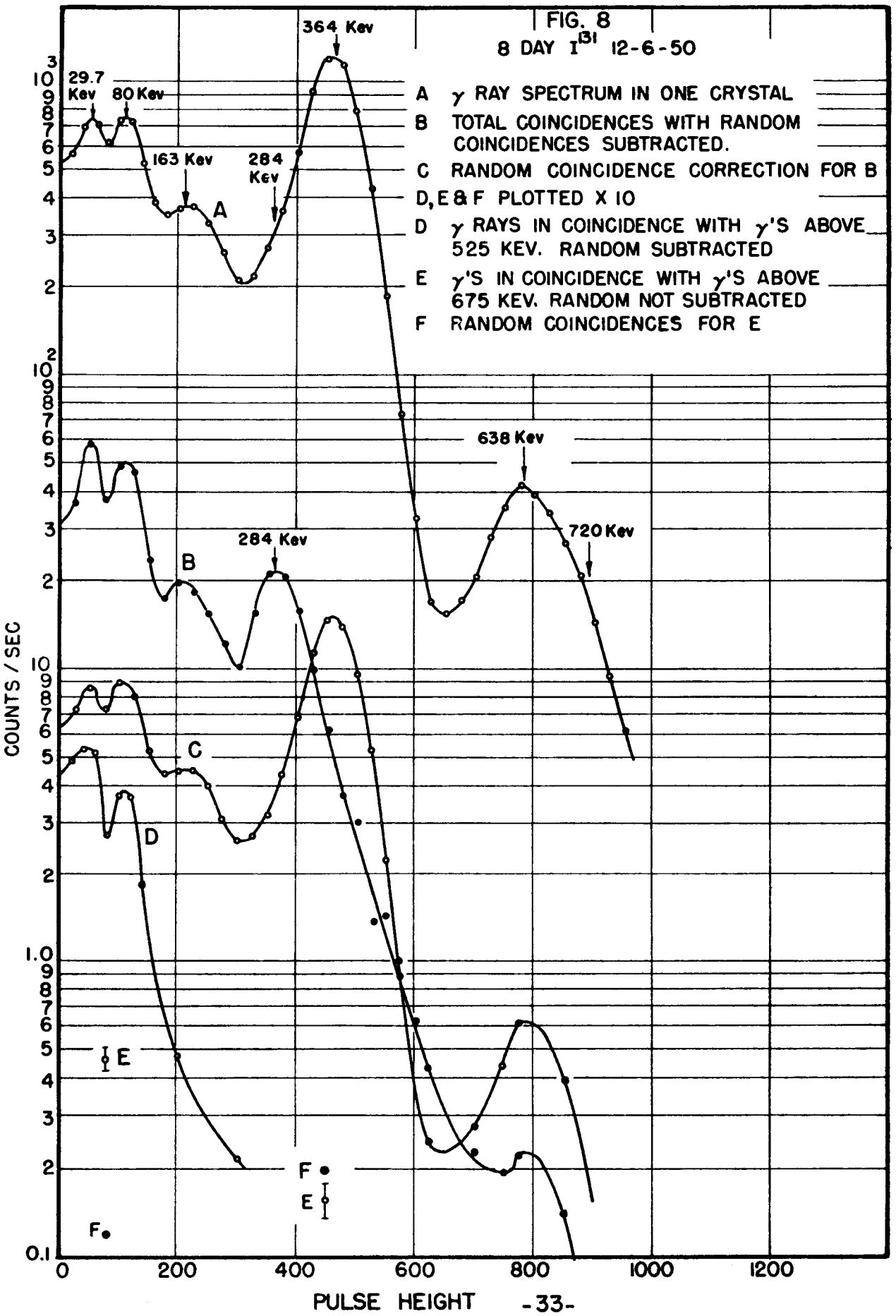

UNCLASSIFIED
DWG. 10325

FIG. 9

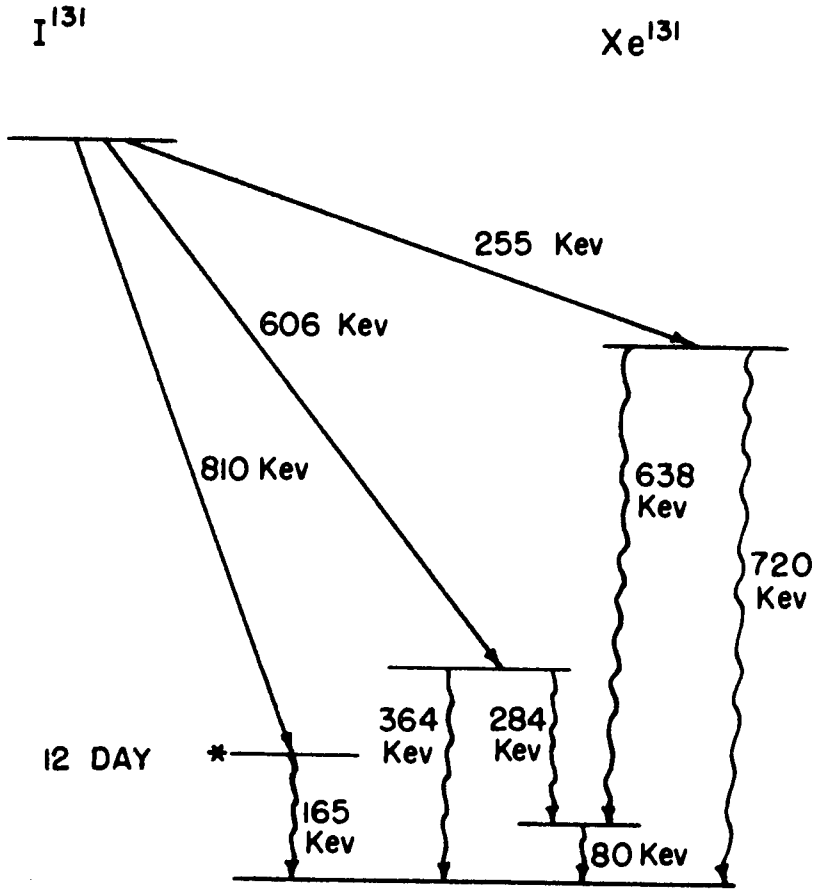

UNCLASSIFIED
DWG.10321

FIG. 10

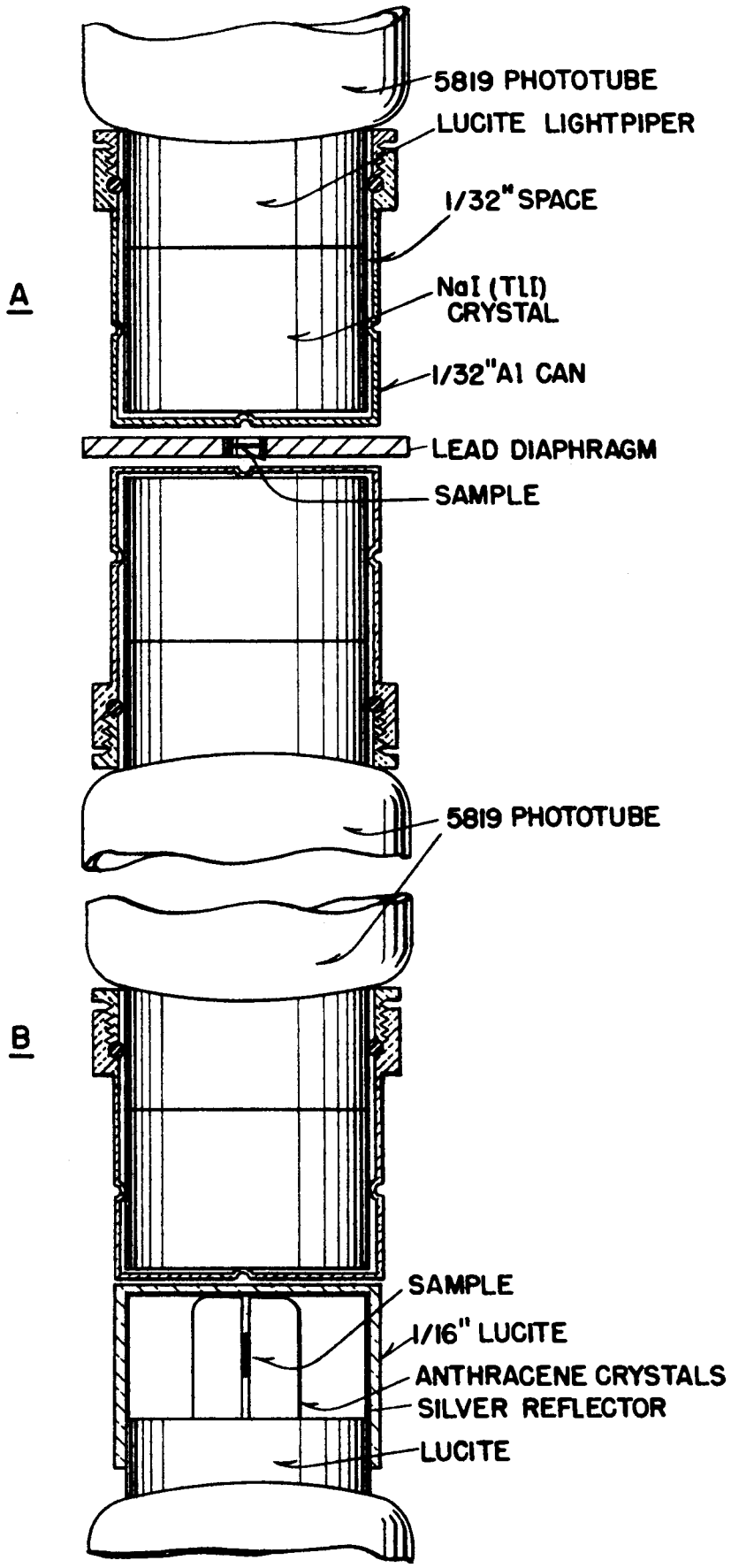

all pulses representing greater than 525 Kev energy, and the spectrum of pulses from the split-crystal spectrometer that are in coincidence with the gamma rays was measured. Figure 11, curve *A*, shows the very peculiar Fermi-Kurie plot obtained. This is, unfortunately, due to the 4π geometry of the split-crystal spectrometer. The inner beta ray is, of course, in coincidence with the 638-, 720-, and 80-Kev gamma rays. The 80-Kev gamma ray is highly internally converted so that if a beta ray is emitted, a coincident conversion electron is often emitted and the amplifier gives a pulse equal to the sum of their energies. The xenon X rays accompanying the conversion electrons are also detected in the anthracene with good efficiency so that any beta ray whose following 80-Kev gamma ray is converted will have an energy 80 Kev greater than expected. The 80-Kev gamma ray itself is also detected with fair efficiency and adds to the number of beta rays displaced upward 80 Kev. After 80 Kev was subtracted from the energy of each point in the beta coincidence spectrum, the Kurie plot was remade and curve *B* resulted. The last 80 Kev of this spectrum should be useful. The beta end point is about 255 ± 10 Kev. To check this result the gamma spectrometer was set up to avoid the 638-Kev gamma-ray pulses. Some of the pulses from the 720-Kev gamma ray remained, and a beta coincidence spectrum was run. Curve *C* shows the result. The statistics are poor on the points since only a few counts remained, but the maximum energy is 255 ± 10 Kev. These values agree well with the value 248 to 252 Kev obtained from various published values.[3]

Hollow-crystal Spectrometer. The difficulties found upon occasion with the split-crystal spectrometer, caused solely by its property of converting all electrons emitted by the sample, cause some concern. As long as all particles are counted, coincident beta rays or beta rays and conversion electrons result in a distorted spectrum. The ordinary scintillation spectrometer, even when using anthracene, gives much poorer Kurie plots than the split crystal owing to the scattering out of beta rays before their whole energy is lost, thereby producing a small pulse where a larger one should be. This effect is prevented in the split crystal, and straight Kurie plots result.

An attempt has been made to get the same effect without leaving the source inside the crystal. A crystal ¾ in. thick and 1 in. in diameter was used. A flat-bottomed hole ¼ in. in diameter and 3/8 in. deep was drilled in

(3) Way, K., *et al.*, *Nuclear Data*, National Bureau of Standards Circular 499, 1950.

UNCLASSIFIED
DWG. 10324

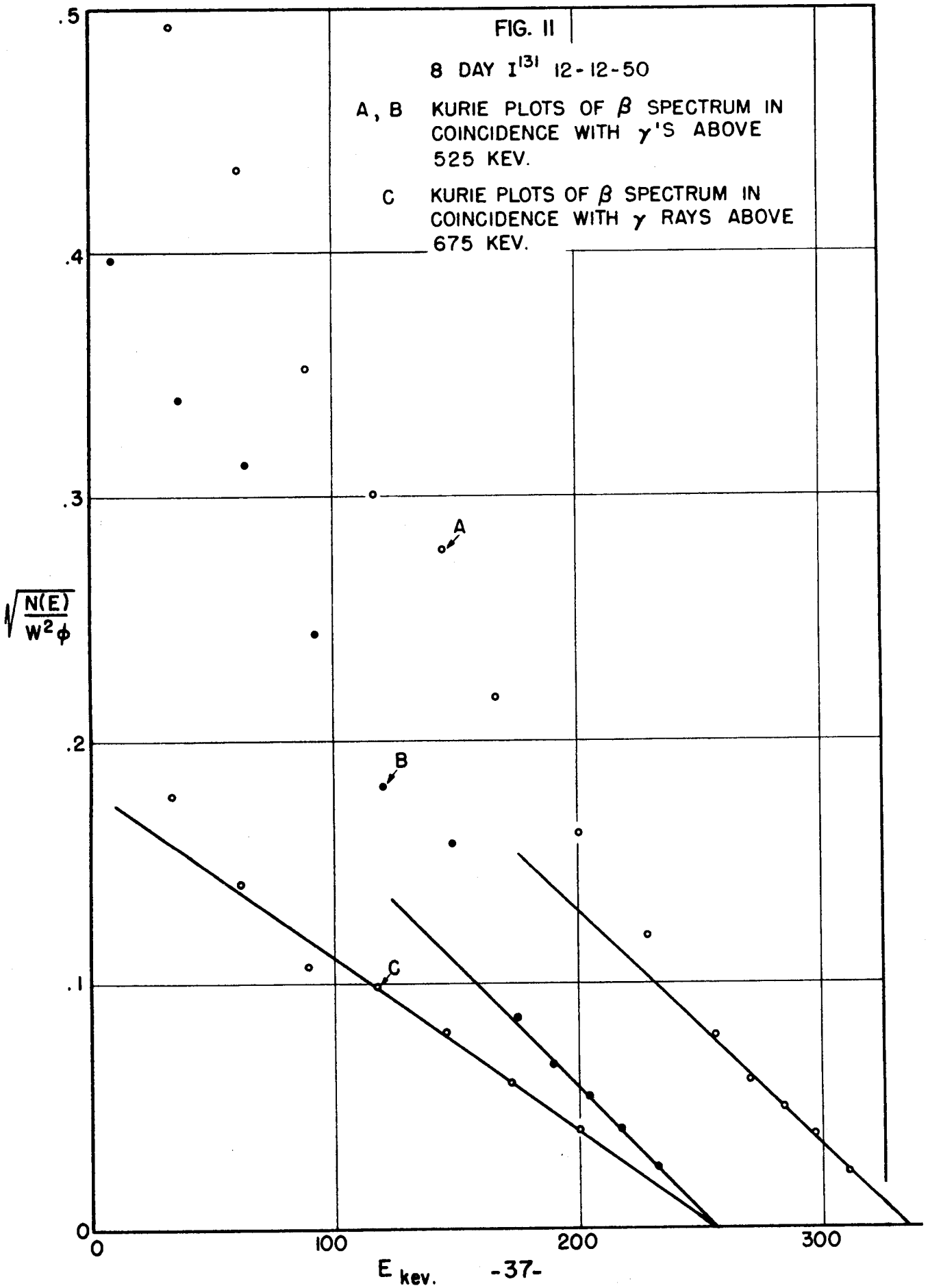

the 1-in.-diameter face using a sharp end mill operated by hand. After polishing with toluene, the undrilled face was cemented to the standard light piper and the crystal and light piper were covered with 0.0002-in. aluminum foil except over the hole, where thinner foil of 0.2 mg/cm^2 was used.

A lucite collimator 5/16 in. thick was placed above the crystal and a P^{32} source on thin film was placed above the collimator so that the beta rays could fall only on the bottom of the hole. It was expected that few of the scattered beta rays would find their way out of the hole after once entering it.

A fairly good spectrum was obtained as shown in Fig. 12. Experiments on this method of spectrometry are continuing.

UNCLASSIFIED
DWG. 10326

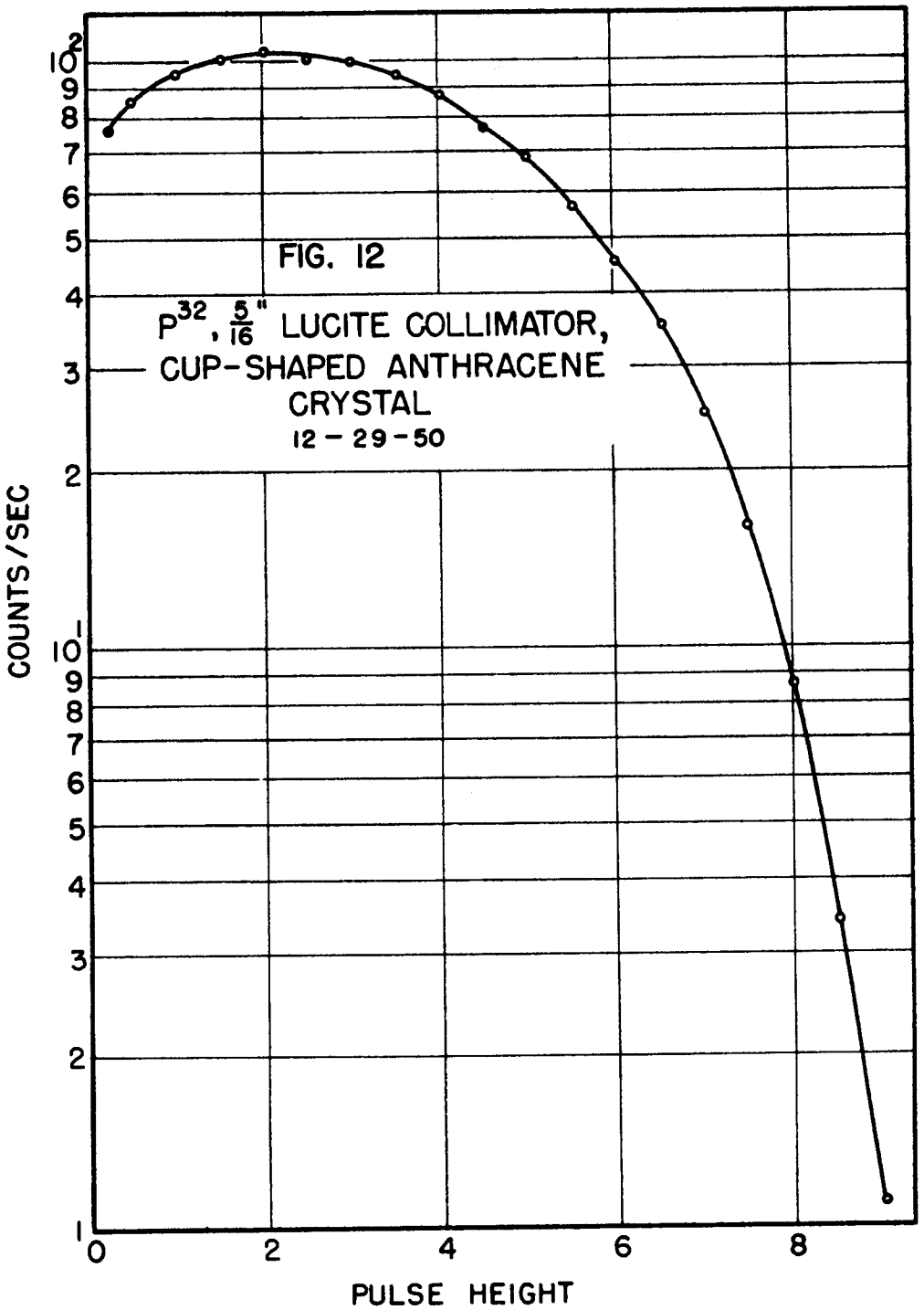

6. ACCELERATOR PROGRAM

W. M. Good G. Robinson
C. D. Moak H. Willard

In the last quarterly report (ORNL-865) preliminary results were given to show the feasibility of employing a scintillation spectrometer to single out gamma rays when several are present and to study them separately. The reaction $B^{11} + H^{1} \longrightarrow C^{12} + \gamma$ furnishes gamma rays of energies of approximately 4, 12, and 16 Mev. This study has been continued to obtain reproducibility, which was previously found to be poor because of troubles with the pulse-height selector and because of certain troubles with the target.

The pulse-height selector previously used has been replaced with a new one after the design of Jordan and Bell of the Physics Electronics Section. This pulse-height selector has given noticeably better reproducibility. It was further found that, with 250 μa on the target, there was build-up on the target of not only carbon, but also aluminum from the aluminum collimators and zinc from the target assembly. The collimators now being used are tantalum, the collimating tube is refrigerated to trap oil from the main accelerator tube, and the target backing is stainless steel. These measures have removed the erratic behavior arising in the target itself. Finally, the accelerating voltage, which is as yet unstabilized, was monitored to keep energy variations down to 1/3 %. This had the effect of keeping the target position more nearly fixed, as did also counterbalancing the rotating counter assembly.

Figure 13 shows the relative intensity of the gamma-ray spectrum versus energy in arbitrary units. The energy interval studied in obtaining the angular distribution of the gamma rays is indicated by the dashed horizontal segment. The resulting angular distribution is shown in Fig. 14. Any interpretation that this angular distribution is that of the 12-Mev gamma ray must await the more detailed study of the spectrum with improved resolution.

UNCLASSIFIED
DWG. 10206

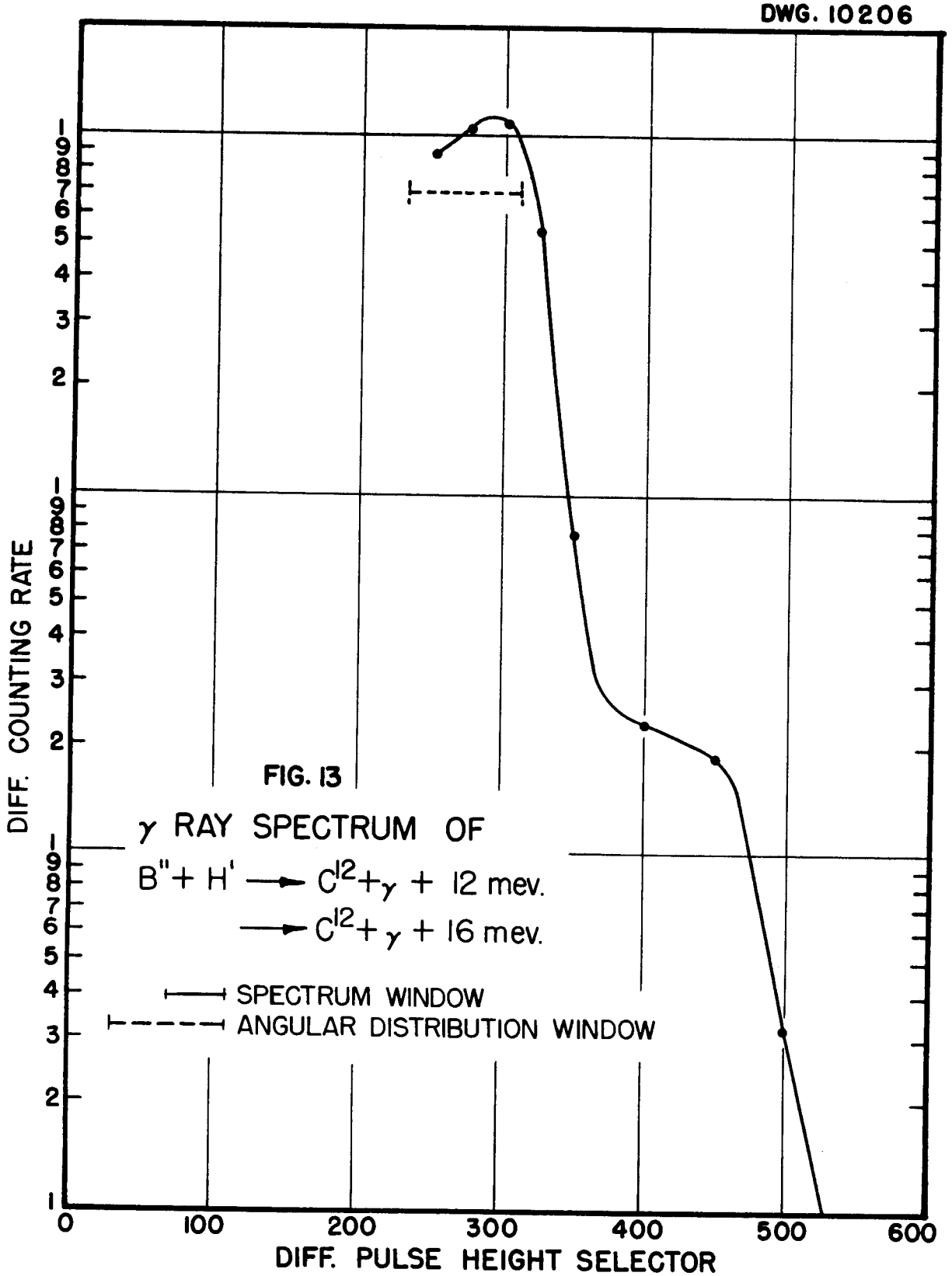

FIG. 13

UNCLASSIFIED
DWG. 10207

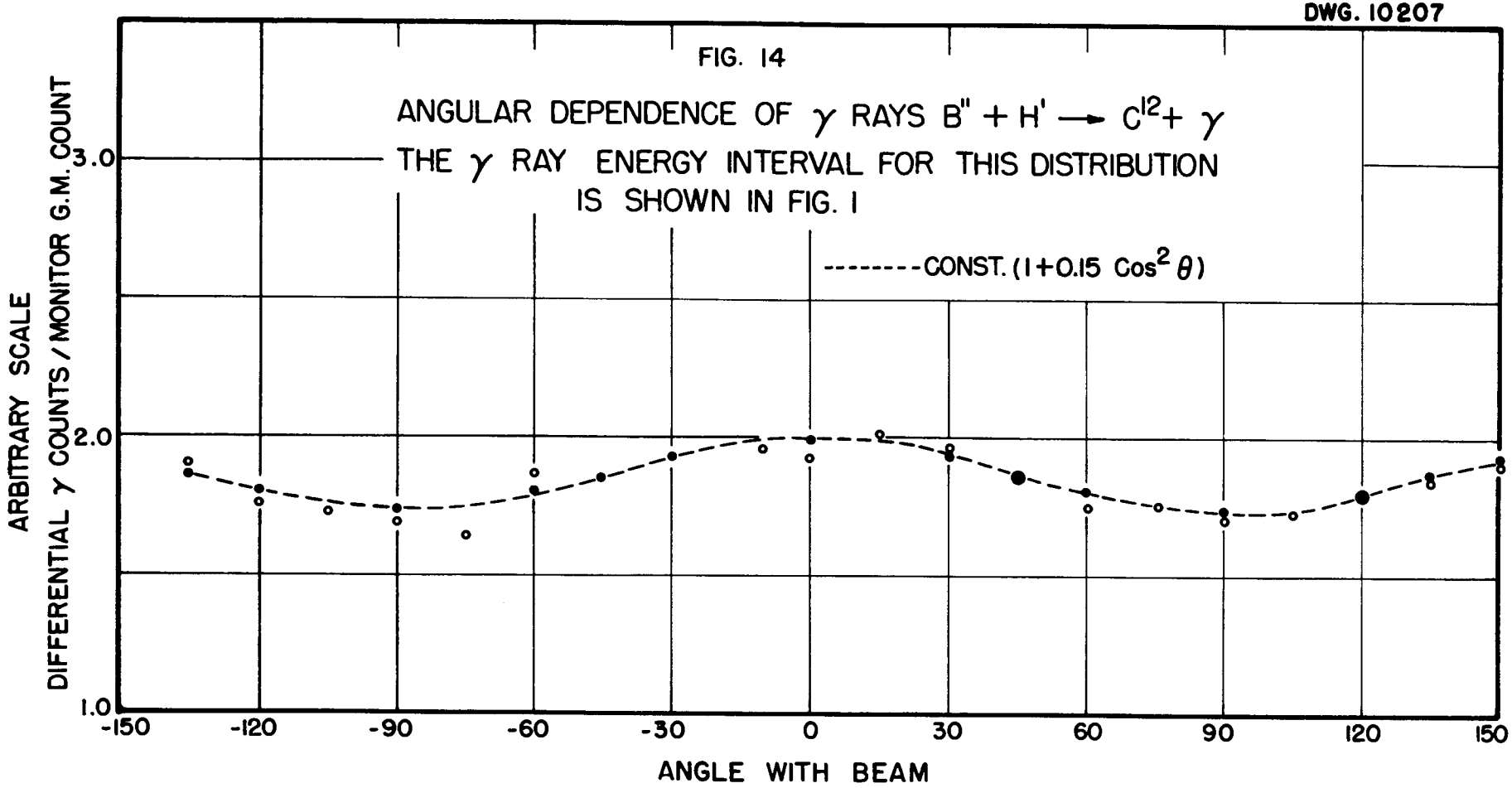

FIG. 14

ANGULAR DEPENDENCE OF γ RAYS $B'' + H' \rightarrow C^{12} + \gamma$

THE γ RAY ENERGY INTERVAL FOR THIS DISTRIBUTION IS SHOWN IN FIG. 1

7. STABLE-ISOTOPE CROSS SECTIONS

H. Pomerance and T. Arnette

The pile oscillator has been used to measure the thermal-neutron cross sections of some stable separated isotopes procured from Y-12. The values given below are based on the value 95 barns for gold using neutrons of 0.025 ev. The errors are estimates based on the sample size and the relative contributions from the other isotopes present in the samples. The chemical analyses were not sensitive enough to rule out boron contributions in the Mg and Si samples, and the possibility of boron cannot be easily included in the estimate of error. The atomic cross sections are obtained by multiplying the nuclear (isotopic) cross sections by the relative abundances.

Cross Sections of Some Stable Isotopes

ISOTOPES		CROSS SECTIONS (barns)	
		ISOTOPIC	ATOMIC
Magnesium	24	0.027 ± 30%	0.027
	25	0.27 ± 30%	0.027
	26	0.06 ± 100%	0.006
Silicon	28	0.08 ± 30%	0.075
	29	0.27 ± 30%	0.012
	30	0.41 ± 100%	0.013
Titanium	46	0.57 ± 30%	0.046
	47	1.62 ± 20%	0.13
	48	7.98 ± 8%	5.86
	49	1.80 ± 25%	0.10
	50	0 ± 0.2	0
Selenium	74	44 ± 20%	0.38
	76	82 ± 10%	7.39
	77	40 ± 10%	3.01
Tellurium	120	70 ± 100%	0.07
	122	2.7 ± 35%	0.07
	123	393 ± 8%	3.49
	124	6.5 ± 20%	0.30
	125	1.5 ± 10%	0.10
	126	0.88 ± 25%	0.14
	128	0.16 ± 100%	0.09
	130	0.53 ± 50%	0.18

For titanium and tellurium the sum of the atomic values can be compared with measurements made with natural material; for the others the value for the natural material was used in the calculations of the isotopic cross sections.

	Sum	Natural
Titanium	6.13*b*	5.83*b*
Tellurium	4.44	4.53

8. NEUTRON ELECTRIC DIPOLE MOMENT

James H. Smith

Work on determining the magnitude or setting an upper limit to the magnitude of the spin-oriented electric dipole moment of the neutron has reached its final stages. No such dipole has been found, but certainly, if any exists, it is less than the electronic charge times 3×10^{-19} cm.

A new iron-mirror polarizer has been installed, and the better polarization it affords will probably allow a limit of 10^{-19} cm to be set on the effective charge separation.

9. THEORETICAL PHYSICS

M. E. Rose and T. A. Welton

Work on the tables of Fermi functions for beta decay is being extended by making tables of correction factors for (1) screening and (2) finite size of the nucleus. The computation of the uncorrected functions has been completed by the computing panel.

A survey of all the experimental literature bearing on angular momentum of excited nuclear states and the multipolarity of emitted gamma radiation is underway.

A Theory of Radiation Widths of Slow-neutron Resonances (T. A. Welton). The radiation widths of all known slow-neutron resonances lie remarkably close to 0.1 ev (within a factor of 2, roughly). This near constancy is quite remarkable in view of the supposed complication of the wave functions for the compound nucleus in its excited and ground states. In the following discussion it will be assumed that the constancy of the width is, in fact, a strong reason for arguing that quantum mechanical details are relatively unimportant in the description of the radiation process. The radiation process will accordingly be described in a simple semiclassical fashion, using only some elementary results of nuclear theory.

We define:

$$\Gamma_r = \hbar w \tag{1}$$

where Γ_r is the radiation width and w is the transition probability per unit time from a state in which the incident neutron is present inside the nucleus with its full incident energy to a state where it has radiated a quantum and is accordingly unable to leave the nucleus. We estimate W classically by arguing that, with the neutron inside the nucleus, the nucleus is largely undisturbed except for the continual interchange of a single "excited" nucleon with other nucleons which form the "undisturbed" structure of the nucleus. On this picture an "excited" neutron is constantly interacting with a proton, or an "excited" proton is interacting with a neutron, either of which processes will cause the emission of electric dipole radiation, accompanying the acceleration of the proton. At the same time the spin of the excited nucleon will

constantly precess because of the spin dependence of the nuclear forces, which process will give rise to the emission of magnetic dipole radiation. The third process to be considered is the emission of electric quadrupole radiation when an excited proton accelerates by interaction with another proton.

We write, in general,

$$w = \frac{1}{\hbar\omega}\frac{dE}{dt} \tag{2}$$

where ω is a mean frequency of the emitted radiation and dE/dt is the classical rate of energy emission. We now specialize Eq. (2) for each of the three radiation mechanisms. For electric dipole radiation, we have

$$\Gamma_{\gamma} = \hbar w = \frac{2e^2}{3c^3}\frac{\overline{|a|^2}}{\omega_n} \tag{3}$$

where $\overline{|a|^2}$ is the mean square acceleration of the excited nucleon and ω_n is a characteristic nuclear frequency. To any accuracy possible here, we can write

$$\left.\begin{aligned} \overline{|a|^2} &= \frac{V^2}{M^2R^2} \\ \omega_n &= \sqrt{\frac{V}{MR^2}} \end{aligned}\right\} \tag{4}$$

where V is an average well depth for the internucleon potential, R is the range of the potential, M is the nucleon mass, and ω_n is evaluated as the reciprocal of the time required for two nucleons to accelerate to coincidence when they start from rest a distance R apart.

We use the relations, where m is the electron mass,

$$R = \frac{1}{2}\frac{e^2}{mc^2}$$

$$2mc^2 = 10^6 \text{ ev}$$

$$\frac{V}{Mc^2} = \frac{40}{1000} = 0.04$$

and obtain

$$\Gamma_r = \frac{2e^2}{3c^3}\frac{V^2}{M^2R^2}\sqrt{\frac{MR^2}{V}}$$

$$\approx \frac{e^2}{R}\left[\frac{\omega_n R}{c}\right]^3 \tag{5}$$

From above,

$$\frac{e^2}{R} = 10^6 \text{ ev}$$

$$\frac{\omega_n R}{c} = \sqrt{\frac{V}{Mc^2}} = 0.2$$

so that Γ_r = 8000 ev. This result is higher than the correct one by a factor of nearly 10^5, and we must tentatively argue that electric dipole radiation is greatly reduced by a mechanism not yet clear.

The Γ_r resulting from magnetic dipole radiation is easily estimated in an analogous fashion. We then have

$$\Gamma_r = \frac{2}{3c^3}\frac{\overline{|\ddot{M}|^2}}{\omega_s} \tag{6}$$

where ω_s is a characteristic spin precession frequency and $\overline{|\ddot{M}|^2}$ is the mean square value of the second time derivative of the magnetic moment of the precessing spin. To the accuracy of the preceding work, we write

$$\overline{|\ddot{M}|^2} = \omega_s^4\left[\frac{e\hbar}{Mc}\right]^2$$

$$\hbar\omega_s = 5mc^2 = 2.5 \text{ Mev} \tag{7}$$

where $e\hbar/Mc$ is approximately the static moment of the nucleon and $\hbar\omega_s$ is taken to be approximately the difference between singlet and triplet deuteron

energies. We then have

$$\Gamma_r = \frac{\omega_s^3}{c^3}\left[\frac{e\hbar}{Mc}\right]^2 = \frac{e^2}{R}\left[\frac{\omega_s R}{c}\right]^3\left[\frac{\hbar}{McR}\right]^2$$

$$= 10^6\left[5\frac{mcR}{\hbar}\right]^3\left[\frac{\hbar}{McR}\right]^2$$

$$= 10^6 \times 125 \times \frac{mcR}{\hbar}\left[\frac{m}{M}\right]^2$$

$$= 1.25 \times 10^8 \times \frac{1}{2 \times 137}\frac{1}{(1840)^2} = 0.13 \text{ ev} \tag{8}$$

which agrees quite well with experiment.

Finally, we estimate the Γ_r arising from electric quadrupole radiation. We have:

$$\Gamma_r = \frac{e^2}{32c^5\omega_n}\overline{|(\dddot{x}^2)|^2} \tag{9}$$

where ω_n is the previously defined nuclear frequency and $\overline{|(\dddot{x}^2)|^2}$ is the mean square value of the third time derivative of the squared interproton distance. To our accuracy we have

$$\overline{|(\dddot{x}^2)|^2} = \omega_n^6 R^4 \tag{10}$$

and therefore

$$\Gamma_r = \frac{1}{32}\frac{e^2}{R}\left[\frac{\omega_n R}{c}\right]^5$$

$$= \frac{1}{32} \times 10^6 \times (0.2)^5 = 1.0 \text{ ev}$$

This width is too large by a factor of 10. In extenuation, it must be pointed out that the parameter $\omega_n R/c$ here enters to the fifth power, and the result is easily reduced to 0.1 ev by a slight decrease in this parameter. This reduction would not appreciably help the gross disagreement obtained in the electric dipole case.

We then tentatively conclude that the radiation widths are to be explained on the basis of magnetic dipole and electric quadrupole radiation, which arises in a simple semiclassical manner. We expect that the radiation widths will not vary appreciably with neutron energy over a range of perhaps a million volts. We further expect that radiation widths with proton bombardment should also be about 0.1 ev. We can make a further prediction that Γ_r should continue to be about 0.1 ev even for nuclei of rather low mass number (but greater than 20, for example).

We must postulate a mechanism for suppressing to high accuracy (1 part in 10^5) the electric dipole radiation to be expected when a proton and a neutron interact. Levinger and Bethe[1] suggest in this connection that the systematic adherence to the alpha-particle model would accomplish the desired suppression. We cannot agree that this mechanism is at all applicable to the situation in question. The alpha-particle model cannot give a complete description even of the ground states of heavy nuclei, for which $A > 2Z$. For the states arising from the introduction of an excited particle, the alpha-particle model seems even less appropriate. It is felt that the desired mechanism must lie in the nature of the neutron-proton force. A possible assumption is that the exchange character of the force is such that interchange of neutron-proton identity occurs with such frequency that the dipole moment oscillates with frequency too high to give radiation of energies of nuclear magnitude. This proposal is being pursued further.

The De Groot—Tolhoek Symmetry Principle in β Decay (L. C. Biedenharn and M. E. Rose). A recent paper[2] in *Physica* examined the consequences of the following symmetry principle:

> "The processes of negatron and positron emission must be symmetrical, apart from Coulomb interactions, in such a way that, if this Coulomb interaction is neglected, the expressions for H_β^- and H_β^+ are equal (possibly with exception of the sign) in any two cases of negatron and positron emission in which the wave functions of the emitted (positive and negative) electrons and neutrinos are physically equivalent and if, further, $\psi_f(p)$ and $\psi_i(n)$ for negatron emission are respectively the same as $\psi_f(n)$ and $\psi_i(p)$ for positron emission."

Despite the many premises in this principle, it is intrinsically believable since positrons should not be distinguishable from negatrons in the absence of

(2) Groot, S. R. de, and Tolhoek, H. A., "On the Theory of Beta Radioactivity. I. The Use of Linear Combinations of Invariants in the Interaction Hamiltonian," *Physica*, 16, 456, especially p. 470 (1950).

electromagnetic interactions. Yet, since the original paper of Fierz in 1937, the contrary has been the (theoretical) conclusion (for theories that mix interactions S with V and/or A with T). Using the notation of De Groot and Tolhoek, the spectra in the case of zero nuclear charge should vary as follows:

$$P_{\pm}(E) = (G^2/2\pi^3)pEq^2[(C_1^2 + C_2^2)\ |\int 1|^2 + (C_3^2 + C_4^2)\ |\int\sigma|^2 + C_5^2\ |\int\beta\gamma_5|^2 \mp (2/E)(C_1C_2\ |\int 1|^2 + C_3C_4\ |\int\sigma|^2)] \tag{1}$$

where they define the C_i's as the constants for mixing the covariants ($1 = S$, $2 = V$, $3 = T$, $4 = A$, $5 = P$) and the integrals denote the nuclear matrix elements. The plus sign refers to positrons, the minus sign to negatrons. The $1/E$ term distinguishes the spectra. To eliminate this difficulty, De Groot and Tolhoek postulate their symmetry principle and draw the conclusion that only (S,A,P) or (V,T) can be mixed.

We have reinvestigated this problem and come to different conclusions, namely:

1. The symmetry principle is contained in the requirement that the usual formulation of β decay be invariant to the extended Lorentz group — in particular, to time reflection.

2. The conclusion that either (S,A,P) or (V,T) may mix is a result of the unduly restrictive reality requirement that De Groot and Tolhoek impose on the covariants.

The requirement of relativistic invariance for the β-decay interaction Hamiltonian is the basic guidepost of the theory. For investigation of invariance for the extended Lorentz group, we must first investigate the properties of Dirac particles under time reflection. This has been done, and the results have been submitted for publication as a letter in *Physical Review*. For our present problem we need only the result that the correct operator for time reversal is $\gamma^1\gamma^3K_0$ where $K_0 \equiv$ complex conjugation.

The symmetry principle has the result that $\gamma^2K_0\ A_k\ \gamma^2K_0 = \epsilon_k A_k$ (γ^2K_0 is the charge conjugation operator and the A_k's are the covariant operators for β decay) where $\epsilon = \pm 1$ and must be the same for the covariants A_k to mix. If, as De Groot and Tolhoek have done, the additional requirement that $\psi^+A_k\psi$ be

real is made, then we find that the only groups that satisfy both requirements are (S,A,P) and (V,T). But the reality requirement is unnecessary; the only necessary reality requirement is that the interaction Hamiltonian invariant be real. Under time reversal it is readily shown that H_β(creation) $\longrightarrow H_\beta^*$ (annihilation) so that for invariance we need $H = H_\beta + H_\beta^*$. Invariance to the extended group therefore implies reality for H and, as a result, we can always satisfy the symmetry principle for any combination of covariants. Therefore, the choice of an interaction in β decay is as wide open as it was before.

A report is planned which will give the above arguments in detail, along with results from the investigation of time reversal in the Dirac theory.

Elastic Scattering of Atoms by Atoms (Stephen Tamor). The elastic scattering of atoms by atoms is being investigated in the energy region of 20 ev to 1 Mev. The interaction is approximated by a screened Coulomb potential of the form $\frac{Z_1 Z_2 e^2}{r} e^{-r/a}$. In this energy region the Born approximation is not valid except for extremely small angle scattering. However, the problem seems to be ideally suited for a classical orbit calculation since, at these energies, the De Broglie wavelength of the atom is much smaller than the screening radius.

Cross sections are being computed numerically for atoms of $Z \approx 10$. These results will be compared with the data of Evans and Stier (experiment now in progress). The angular distribution will serve as a qualitative check on the correctness of the assumed interaction, while the magnitude of the cross section will enable us to determine the value of the screening parameter a.

10. HEAVY-ION RESEARCH

G. E. Evans P. M. Stier
V. DiRito

A large proportion of the time of this group during the last quarter has been spent in the design and construction of experimental equipment, which will be used in conjunction with Cockcroft-Walton accelerator facilities. An additional accelerator tube for the use of this group is being erected by the high-voltage group, and should be available for experimental use early in the next quarter.

The furnace-type ion source previously reported (last quarterly report) has been rebuilt to improve beam stability and is being bench-tested. A target assembly has been constructed which will allow bombardment of radioactive metal targets with an ion beam. Any metal sputtered from the target surface by the beam will be collected on cooled fins and counted. The deterioration of target surfaces will be studied by varying the energy and type of ion beam and the type and temperature of the target. An instrument which will automatically record resistances in the range 0.1 to 1000 ohms has been built and is being calibrated. This instrument will be used to record the resistance of evaporated targets during radiation or heat treatments.

An automatic temperature-controlling device for target assemblies has been designed, and is being built by the instrument shop. This device will hold a target at any temperature from -178°C to +25°C, or will vary the temperature at a controlled rate. The target assembly for low-temperature bombardments has been completed.

A windowless target for gases, employing differential pumping at a series of pinholes, has been designed, and component pumps are on order.

Experiments using the Van de Graaff accelerator have been postponed temporarily during the conversion of the accelerator to a dual polarity machine.